

A perspective on inelastic light scattering spectroscopy for probing transport of collective acoustic excitations

Hyemin Kim ,^a Hyungseok Kim ,^a and Taeyong Kim ,^{1,2,3,b}

¹*Department of Mechanical Engineering,*

Seoul National University, Seoul 08826, Republic of Korea

²*Institute of Advanced Machines and Design,*

Seoul National University, Seoul 08826, Republic of Korea

³*Inter-University Semiconductor Research Center,*

Seoul National University, Seoul 08826, Republic of Korea

Abstract

Understanding and manipulating nanoscale energy transport and conversion processes are essential for diverse applications, ranging from thermoelectrics and energy harvesting to thermal management of microelectronics. While it has long been recognized that acoustic and thermal properties in condensed matters are primarily due to microscopic transport of phonons as quasiparticles, probing thermal acoustic excitations particularly at sub-THz remains a challenge primarily due to limitations in experimental techniques with spatiotemporal resolutions pertinent to probing them. Brillouin light scattering (BLS) and its variant, impulsive stimulated Brillouin scattering (ISS), provide access to these thermal acoustic excitations, enabling measurement of quantities such as acoustic dispersions along with relaxation dynamics occurring in ultrasonic as well as hypersonic frequencies. In this perspective, we provide a brief overview of the operational principles of BLS and ISS, and highlight their applications in probing acoustic, thermal, and magnetic excitations in emerging and low-dimensional materials. We conclude by discussing current challenges and future opportunities for advanced material characterization using Brillouin light scattering spectroscopy techniques.

^a Hyemin Kim and Hyungseok Kim contributed equally to this work.

^b tkkim@snu.ac.kr

INTRODUCTION

Nanoscale energy transport and conversion processes are essential for a wide range of applications in thermoelectrics, energy harvesting, and heat dissipation in modern devices [1–7]. These processes are primarily facilitated by quasiparticles, among which phonons are dominant heat carriers in crystals [8, 9]. On a microscopic scale, lattice heat conduction can be characterized by dispersion relations determined by crystal structure and relaxation dynamics that govern the transport properties of these heat-carrying quasiparticles. It has been demonstrated that long-wavelength, sub-THz thermal acoustic phonons contribute substantially to heat transport in bulk and nanostructured materials [1], and that access to these modes is essential for understanding and tailoring their thermal and acoustic properties. Diverse scattering spectroscopy techniques have been developed and applied to probe the transport of thermal phonons in condensed matters, among which inelastic neutron scattering (INS) and inelastic X-ray scattering (IXS) are well-established methods for measuring vibrational dispersion relations and lifetimes [10–14]. However, since INS requires an ample sample volume ($>\text{mm}^3$ [15]), it has limited sample coverage, especially for specimens that need to be synthesized as thin films, and kinematic constraints complicate measurements even when sufficient sample volume is available. Moreover, the resolution limitations of IXS restrict access to sub-THz vibrations. [16, 17].

To probe thermal acoustic phonons beyond the spectral resolution of INS and IXS, Brillouin light scattering spectroscopy (BLS) has emerged as an established technique, complementing Raman spectroscopy which allows to probe zone-center optical polarizations [18, 19]. In principle, Brillouin scattering, also known as Brillouin–Mandelstam scattering, involves the scattering of an optical wave by an acoustic wave. The earliest theoretical works on Brillouin scattering were independently presented by Brillouin [20] and Mandelstam [21] in the early 20th century. The first experimental observation was reported shortly thereafter by Gross [22, 23]. The subsequent introduction of Fabry-Perot (FP) interferometers by Sandercock [24] became a key component in modern BLS configurations, providing high contrast while maintaining moderate finesse to ensure sufficient transmittance of Brillouin signal for achieving high signal-to-noise ratio. Later, stimulated Brillouin light scattering was developed as a means to efficiently amplify the scattered signal [25] whose intensity by the spontaneous process is known to be substantially weak [26, 27]. The scattering process

can be stimulated through the strong coupling between the incident light and the material, producing an exponentially amplified signal [28]. Building on this, by introducing a pump laser with a pulse duration less than period of oscillation (inverse of acoustic phonon frequencies), the pump pulses impulsively create spatially periodic and time-dependent excitations in the material [29, 30]. The following modulations in the optical properties of the material can be measured using a probe beam. This method, termed impulsive stimulated Brillouin scattering, was demonstrated by Boersch and Eichler in 1967 [31]. We will refer to this process as impulsive stimulated Brillouin scattering (ISS) when the scattering occurs in a stimulated manner by an impulsive light source, whereas we will specify the term Brillouin light scattering when addressing spontaneous or general Brillouin scattering.

Due to its non-contact and non-destructive nature, BLS has been extensively employed for characterizing photoelastic properties of crystalline and glassy materials across a range of phases [32–36]. In addition to elastic measurements, BLS has emerged as a routine tool for probing properties of quasiparticles such as phonons and magnons. In the case of phonons, BLS enables access to low-frequency phonon dispersion, especially in nanosstructured solids. For instance, BLS has been used to observe confined phonon modes in GaAs nanowires [37], and to resolve gigahertz phonon dispersion relations in patterned holey silicon membranes, thereby providing direct experimental evidence of omnidirectional vibrational band gaps in phononic crystals [38]. Beyond acoustic excitations, BLS can also probe magnons, which are of interest for spintronics applications [39–43]. BLS has been employed to spatially map magnon propagation in magnonic waveguides [43–45], to quantify interfacial Dzyaloshinskii-Moriya interaction strength in metal multilayers [41, 46] and, notably, to demonstrate magnon Bose-Einstein condensate at room temperature [47, 48].

Stimulated Brillouin scattering and impulsive stimulated Brillouin scattering extend these capabilities by enhancing the intensity of Brillouin signal. These techniques have been widely applied to study thermal and elastic properties of thin films, suspended membranes, and bulk materials [49–52], as well as highly anisotropic materials and soft matters [53–56]. A key feature of impulsive stimulated Brillouin scattering is its tunable accessible length, which is pertinent to probing transport processes across different spatio-temporal scales. This extends measurements of heat transport beyond the diffusive regime, allowing experimental reconstruction of vibrational mean free paths (MFPs) spectra in lattices with various phases by resolving ballistic heat transport [50, 51, 57, 58]. Additionally, beyond mean free path

spectroscopy, it has been applied to detect second sound in graphite at markedly high temperatures by accessing phonon hydrodynamic transport regime [59, 60]. Another variant of ISS is spin grating spectroscopy, which has been applied to probe electronic spin dynamics and valley polarization dynamics: discovery of spin-Coulomb drag in GaAs quantum wells; observation of the persistent spin helix in semiconductor quantum wells; measurement of valley depolarization dynamics in low-dimensional materials [61–63].

In this mini-review, we provide a brief overview of working principles and instrumentations of modern BLS and its variant, ISS. We then highlight recent studies that employ BLS and ISS to investigate various modes of nanoscale energy transport, including acoustic, thermal, and magnetic excitations. The purpose of this review is to provide an accessible introduction to these photonic techniques, with a perspective on their evolving applications. This manuscript is organized as follows: we first introduce brief operational principles of BLS, and survey its contemporary applications; next, we then present ISS in the same order. This review aims to provide the scientific community with our perspective on current trends and future opportunities for advancing Brillouin light scattering spectroscopy as a versatile tool for characterizing energy transport and conversion across emerging materials and nanoscale systems, extending its scope beyond conventional applications.

I WORKING PRINCIPLES AND INSTRUMENTATION OF BLS

Unlike other inelastic scattering spectroscopies such as inelastic X-ray scattering, which are limited to resolve excitations with frequencies above a few THz, Brillouin scattering offers access to acoustic excitations with frequencies ranging from sub-gigahertz up to several hundred gigahertz, as shown in Fig. 1(a). In this section, we provide a brief introduction on the working principle of Brillouin scattering spectroscopy techniques, and outline modern experimental configurations that enable such spectral resolution in these photonic approaches.

A Stokes and anti-Stokes scattering

Typical BLS spectra exhibit several intensity peaks as shown in Fig. 1(b): a peak with its central frequency identical to that of the incident optical wave as a result of elastic Rayleigh scattering, along with other frequency-shifted (inelastic) peaks demonstrating Stokes shifts.

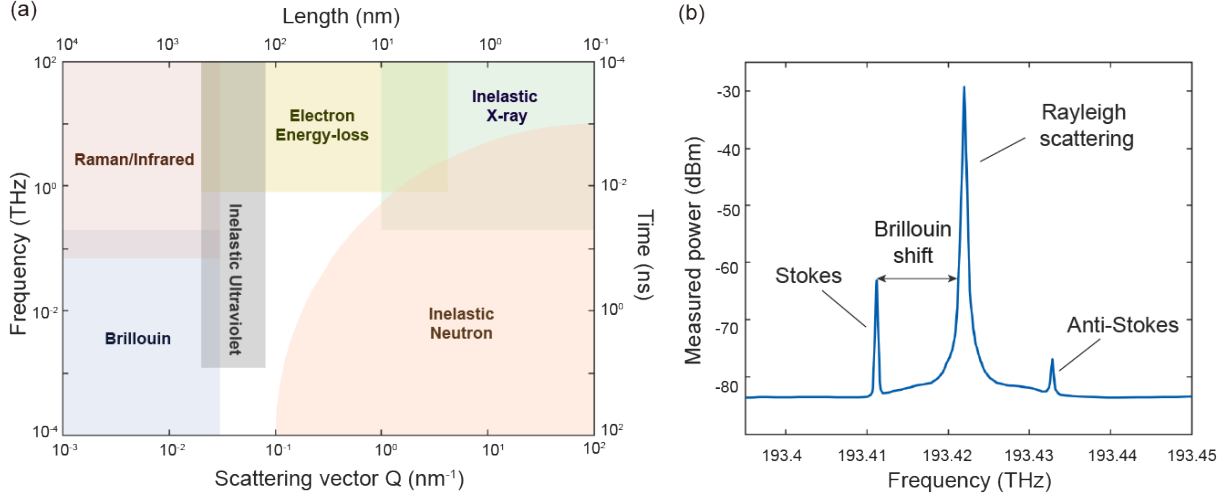


FIG. 1. (a) Map showing the accessible frequency and momentum transfer ranges of different inelastic scattering spectroscopy techniques. Shaded regions indicate typical accessible windows for each technique, and the Brillouin scattering shows the appropriate range to probe excitations with relatively low frequency and momentum. Adapted from Ref. [64] with permission under CC BY license. (b) Representative Brillouin scattering spectra showing inelastic Stokes (downshifted) and anti-Stokes (upshifted) peaks, displaced from the central Rayleigh peak by Brillouin shift. The shifted peaks exhibit relatively low intensity compared to Rayleigh scattering, and the spectral separation is determined by the wavelength and angle of incident light, together with the refractive index and acoustic velocity of a material. Adapted from C. Wolff, M. J. A. Smith, B. Stiller, and C. G. Poulton, "Brillouin light scattering—theory and experiment: tutorial," *J. Opt. Soc. Am. B* **38**, 1243-1269 (2021), <https://doi.org/10.1364/JOSAB.416747>. © 2021 Optica Publishing Group. Used under the terms of the OAPA/CC BY license. [65].

The downshifted component is due to Brillouin scattering in which light is scattered by an interaction with acoustic waves, namely phonons, in the medium. In this process, called the Stokes process, phonons are created during the light-matter interaction, resulting in a lower frequency of the scattered wave. In contrast, the upshifted peak at higher frequency corresponds to the anti-Stokes scattering where phonons are annihilated during the interaction, causing a frequency increase in the scattered light.

The inelastic scattering events should obey energy and momentum conservation between the incident and scattered lights with nearly identical wavevectors due to small momentum

transfer compared to the optical wavevectors \mathbf{k} . The frequency shift of measured lines, which is identical to those of phonons with momentum \mathbf{q} is expressed as [27]

$$\nu = \pm \frac{2n v_s}{\lambda_i} \sin(\theta/2) \quad (1)$$

where λ_i is wavelength of incident optical wave, n is the refractive index, v_s is acoustic velocity, and θ is scattering angle. As can be seen in Eq. 1, it is apparent that the magnitude of the frequency shift is maximum (minimum) at scattering angle of $180^\circ(0^\circ)$. This indicates that backscattering geometry ($\theta = 180^\circ$) provides access to the maximum detectable phonon wavevector along with the corresponding frequency, while spectrum of forward scattering will be dominated by Rayleigh scattering due to the smaller momentum transfer. The frequency shift in Brillouin scattering can also be interpreted as a Doppler effect between light and the acoustic wave. More precisely, the redshift observed in Stokes scattering is analogous to light scattering from a receding acoustic wave in the material, while the blueshift of the scattered wave in anti-Stokes scattering corresponds to scattering from an approaching acoustic wave [27, 66].

An additional physical property can be extracted from analyzing the peak widths of BLS spectra. As shown in the peaks of Fig. 1(b), shifted peaks manifest a finite width due to acoustic attenuation. The linewidths of the peaks are directly related to the phonon lifetimes, where phonon lifetime τ_p can be determined using full width at half maximum (FWHM) of the Brillouin peak using $\Delta\nu = 1/\Delta(2\pi\tau_p) = \Gamma|\mathbf{q}|^2/2\pi$. Here, $\Delta\nu$ is the FWHM and Γ is the attenuation coefficient [67]. Noting that the momentum transfer is $|\mathbf{q}| = 2|\mathbf{k}| \sin(\theta/2)$, lifetime is determined as follows [27].

$$\tau_p = \frac{1}{4\Gamma|\mathbf{k}|^2 \sin^2(\theta/2)} = \frac{\lambda_i^2}{16n^2\pi^2\Gamma \sin^2(\theta/2)} \quad (2)$$

From Eq. 2, the width of Brillouin peaks directly reflects the lifetimes of phonons which participate in the scattering process, and provides insight into the transport properties of low-energy phonons in the material along with the physical properties such as elastic constants. For example, in liquids, sub-ns vibrational lifetimes at a few gigahertz were measured in toluene and methylene chloride, and the results reflect the viscosity coefficients of such media [68]. The vibrational lifetimes in several glasses were estimated to be in the range of 2-4 ns at hypersonic frequencies, falling between the values of organic liquids and crystalline quartz, where the latter exhibits a phonon lifetime of ~ 5 ns [69]. Given that

lifetimes of acoustic vibrations in glasses lie between those of crystals and liquids, it indicates that vibrational lifetimes depend on the underlying lattice structure and phase of a material.

B Spontaneous Brillouin scattering spectroscopy

In principle, Stokes and anti-Stokes scattering of spontaneous Brillouin scattering are driven by modulations in the dielectric constant due to thermal fluctuations and zero-point energy [26, 27]. Such variations in the optical properties lead to inelastic scattering of the incident light, and two types of excitations are involved depending on the optical characteristics of the materials. In weakly absorbing materials such as optically transparent or semitransparent media, where their optical penetration depth is sufficiently larger than the wavelength of incident light, the BLS signal primarily arises from bulk phonons via opto-elastic coupling [70]. In opaque or strongly absorbing materials, if penetration depth is limited to the surface due to high optical extinction of the medium, scattering predominantly occurs by surface phonons [71]. In either case, the magnitude of the measured phonon wavevector depends on the incident angle and the wavelength of the excitation laser as described in Eq. 1.

A schematic of a representative experimental setup used for backscattering BLS is shown in Fig. 2(a). A laser beam is initially directed toward a beam splitter, where the reflected light is used to define a zero-frequency position for calibrating 3FP interferometers. The transmitted beam is refined by a polarizer, then its polarization is adjusted by a half-wave plate to enhance sensitivity to the quasiparticle mode of interest [72]. The sample is typically mounted on a motorized rotation stage to vary the incidence angle of the laser [73, 74], which provides access to different phonon wavevectors in opaque samples, whereas in bulk transparent materials, phonon wavevector is determined by the refractive index of the medium as $|\mathbf{q}| = 4\pi n/\lambda_i$ in backscattering geometry [75]. The scattered light is then focused into FP interferometers, which provide a high spectral contrast to isolate weak Brillouin peaks from strong elastic Rayleigh line while suppressing parasitic transmission peaks and maintaining high effective transmittance via tandem design of interferometers [76]. The output is detected by a photomultiplier tube in single-photon counting mode to capture low-intensity scattered light. With sub-GHz spectral resolution, modern BLS configuration can detect weak optical signals, which allows access to hypersonic phonons and thermal magnons [76, 77], even in thin film with a few Angstroms [78]. Another advantage of such

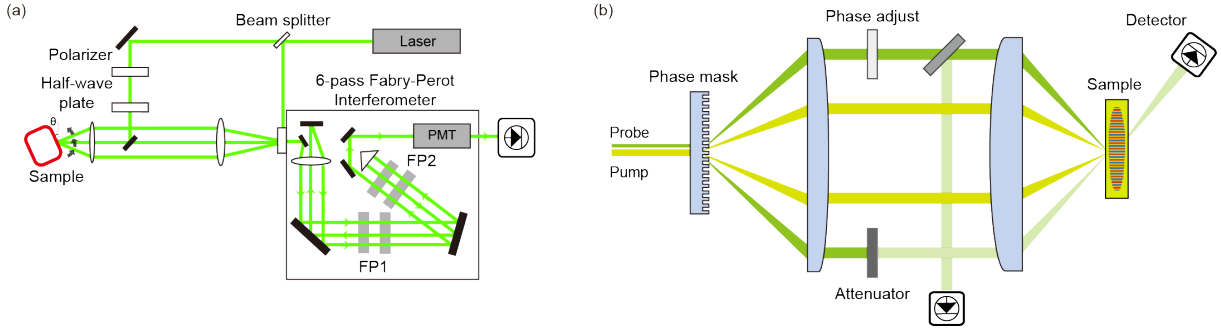


FIG. 2. Typical experimental setup for (a) spontaneous Brillouin light scattering spectroscopy, adapted with permission from DOI:10.1088/0022-3727/45/27/275302, *J. Phys. D: Appl. Phys.*, **45**, 275302. Copyright 2012 IOP Publishing Ltd [83], and (b) impulsive stimulated scattering spectroscopy.

configuration is automation via self-aligning FP interferometers [79], allowing versatility in typical lab settings. Adding an objective lens with a high numerical aperture to achieve small laser spot and integrating an automated 3D scanning stage yield micro-focused BLS, or μ -BLS, which has been used for spatiotemporal imaging of surface phonon and spin waves [80–82].

II APPLICATIONS OF BLS

Conventionally, one of the earliest and continuing applications of BLS is characterizing elastic properties such as sound velocities and elastic moduli of materials [85–88], particularly bulk crystals and minerals under high pressures up to ~ 64 GPa and temperatures above 1800 K [87, 89–92], where traditional mechanical testing is challenging to apply and only feasible up to a few GPa due to large sample size constraints and difficulties in ensuring sufficient transducer-sample adhesion [93–96].

More recently, Brillouin spectroscopy has been employed to characterize elastic properties of novel materials, including soft lattices of hybrid halide perovskites [32, 84]; as shown in variations in Brillouin shifts from hybrid perovskites with different ionic compositions in Fig. 3(a), it was demonstrated that adjusting cation and halide composition can stiffen their lattices [84]. BLS has also been applied to complex crystals [74, 97–100], where a recent study used Brillouin scattering to obtain an elastic tensor of a topological insulator (Sb_2Te_3), resolving its out-of-plane elastic constant c_{33} by measuring velocity of surface

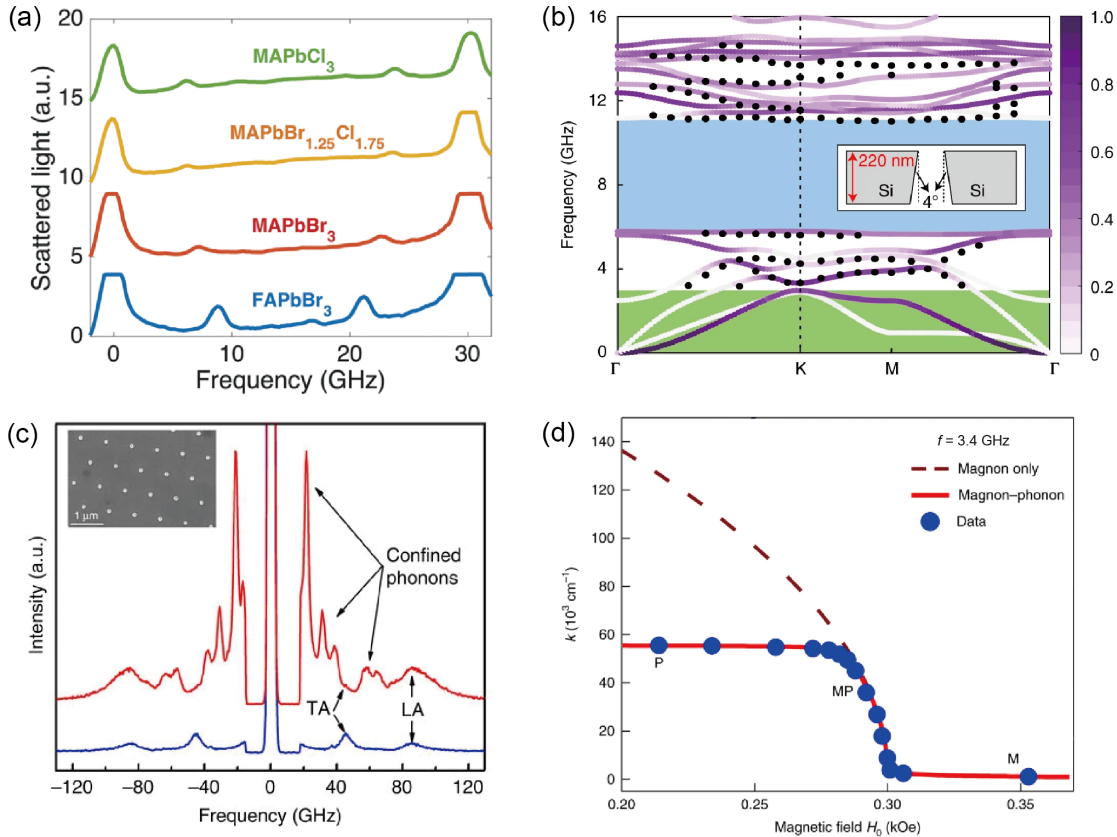


FIG. 3. (a) Comparison of Brillouin spectra for hybrid halide perovskites with different cations and halides compositions, showing larger Brillouin shifts with increasing MA and Cl content. Reproduced from Ref. [84] with permission from the Royal Society of Chemistry. (b) Phonon dispersion relation in a holey Si membrane obtained from BLS compared with simulations, showing an omnidirectional band gap [38]. Reprinted with permission from Florez, O. et al. Nature Nanotechnol. 17, 947-951 (2022). Copyright 2022 Springer Nature. (c) Measured Brillouin spectra of GaAs nanowires array (red) compared to bulk GaAs substrate (blue), showing additional low-frequency peaks corresponding to confined acoustic phonon modes. Reproduced from Ref. [37], licensed under a Creative Commons Attribution 4.0 International License. (d) Wavenumber-resolved BLS signal from a YIG thin film, showing field positions of maximum BLS amplitude, which corresponds to hybridized magnon-phonon modes. [42]. Adapted with permission from J. Holanda et al. Nature Phys. 14, 500-506 (2018). Copyright 2018 Springer Nature.

acoustic modes [101]. Likewise, BLS has been applied to 2D layered crystalline materials and polycrystalline thin films to measure elastic anisotropy [102–105]. For instance, in few-layer MoSe₂ membranes, BLS was used to detect a $\sim 30\%$ reduction in their in-plane stiffness compared to bulk, confirming elastic softening as the number of layers decreases [106]. Extending its scope, theoretical work has proposed that Brillouin scattering could provide access to Majorana fermions and other low-energy boundary modes arising in quantum spin liquids, in particular α -RuCl₃ 2D honeycomb structure, where these excitations are inaccessible using standard experimental probes such as angle-resolved photoemission spectroscopy due to their chargeless nature [107].

In addition to elastic property measurements, BLS has also become an indispensable method for probing dispersion relations and lifetimes of gigahertz vibrational modes in nanostructures and phononic crystals [38, 108–115]. In periodic nanostructured solids, BLS can directly observe phenomena such as Bragg band gaps, zone folding of acoustic phonon branches, and localized resonant modes [110, 111, 116]. It is generally accepted that in surface acoustic waves, periodically arranged scatterers (holey structure) cause phonon band folding and Bragg gaps [38], as shown in Fig. 3(b), while periodic arrays of local resonator (pillar-based) structures introduce additional low-frequency gaps [117, 118]. Another interesting phenomenon in nanostructures is phonon confinement induced by boundary conditions, leading to modified phonon dispersion that can affect thermal conductivity [119–123]. As demonstrated in Fig. 3(c), BLS was employed to observe multiple acoustic phonon subbands in free-standing GaAs nanowires, confirming the existence of confined phonon modes in structures with length scales on the order of hundred nanometer [37].

Another class of quasiparticles accessible by BLS are spin waves, also known as magnons. In magnetic thin films and multilayer heterostructures, BLS is one of the established techniques to measure dispersion relations and damping of spin waves [34, 124–128]. BLS has been used to spatially map the intensity of the Brillouin peak due to magnons under external magnetic field, thereby measuring the decay length of spin waves in thin metal strips [39, 129, 130]. Magnetoelastic waves are another area of interest, in which BLS has been employed to probe magnon-phonon interactions [131–134], demonstrating magnon-phonon conversion that yields a plateau in the field position since phonon modes are independent of the external magnetic field, as shown in Fig. 3(d), and further revealing that spin angular momentum can be transferred from magnons to phonons [42]. Analogous to

phonons, magnon confinement effects were observed using BLS and μ -BLS in metallic thin films [135–138], highlighting possible strategies to manipulate magnon transport for spintronics applications.

III WORKING PRINCIPLES AND INSTRUMENTATION OF ISS

Impulsive stimulated light scattering is a method that probes light scattering using impulsive pump-probe setups to detect the transport and relaxation processes of energy carriers such as phonons and electrons [139]. The scattering can be stimulated when the acoustic wave in a material is induced through the excitation process with the incident light.

The excitation process through the interaction of the laser and acoustic waves in a material is explained by two primary mechanisms: electrostriction and optical absorption. First, electrostriction is a mechanism in which mechanical stress in materials varies under an applied electric field, thereby enabling the stimulated scattering in non-absorptive materials [140, 141]. Second, photothermal excitation can occur in absorbing materials [69, 142], where optical absorption leads to localized heating and subsequent thermal expansion [27]. In general, the stimulated stress in a sample is generated by a combination of both electrostriction and absorptive effects, with the relative contribution of each mechanism depending on the properties of the material.

In non-absorptive media, Brillouin scattering process can be stimulated through the process of electrostriction. Impulsive stimulated Brillouin scattering (ISBS) is an excitation mechanism that utilizes electrostriction to generate dynamic gratings. The interference pattern modulates dielectric properties at regions of high electric field intensity, inducing a periodic density grating through electrostriction [140, 141]. This density wave propagates at the material's sound velocity, with stress profiles that can be described by an impulse response. The generated acoustic waves exhibit dependence on the material's intrinsic viscoelastic properties through their velocity and attenuation characteristics [143].

On the other hand, for absorptive media, impulsive stimulated thermal scattering (ISTS) can measure acoustic properties of materials from their response to impulsive photothermal excitation [144]. Incident optical beams excite the electrons, which, subsequently thermalize through recombination and scattering processes with the lattice, imparting their energy to phonons. This non-radiative recombination process of excited electrons dissipates energy

as heat through phonons and includes the relaxation process after the Auger and Shockley–Read–Hall (trap-assisted) recombination. As a result, following the intensity grating of incident beams, a spatially periodic transient temperature profile is formed [145]. The resulting thermal expansion produces a subsequent stress, which launches counter-propagating coherent acoustic waves [146].

As an experimental method for measuring scattered light, ISS can be utilized in the form of transient grating spectroscopy (TGS). TGS is a simplified variant of four-wave mixing that employs two temporally coincident, coherent pump beams crossed at an angle to generate a spatially modulated excitation field in a sample. The interference between these two coherently superimposed optical pump waves creates a spatially periodic interference pattern, which can then be measured by probe beams [145]. Through variations in the real and imaginary refractive indices n and k , the interference pattern generates phase and amplitude transient gratings, respectively, and the detector observes the probe beam diffracted from these gratings.

Contemporary TGS configuration that involves the phase mask and implements heterodyne detection is presented in Fig. 2(b). Heterodyne detection is a phase-sensitive detection technique that mixes the diffracted beam with a reference beam [147]. It offers advantages in achieving a high signal-to-noise ratio by suppressing unwanted noise components, while not saturating the detector. The first-order diffracted beams from the phase mask are selected as probe beams. One beam then passes through an optical phase adjust and acts as the signal beam to detect material properties, while the other beam is attenuated and employed as the reference beam in heterodyne detection. After Bragg diffraction of the signal beam at the sample, the diffracted signal beam is now superimposed onto the reflected or transmitted reference beam, depending on whether reflection or transmission geometry is used. For a thin sample under the transmission geometry, the intensity of the first-order diffracted probe beam under direct (homodyne) detection, assuming small refractive index modulation, is given by [139]

$$I_{\text{df},t} = I_{\text{sig,td}} \left[(\Delta n)^2 + (\Delta k)^2 \right] \quad (3)$$

where Δn and Δk are the amplitude and phase grating signal caused by the real and imaginary parts of the refractive index respectively, and $I_{\text{sig,td}}$ is the intensity of signal beam transmitted through the specimen in the presence of the thermal grating. In contrast,

the time-dependent signal intensity from the heterodyne detection is

$$I_{\text{hd},t} = I_{\text{sig,td}} 2t_r [\Delta n \sin \Delta\phi - \Delta k \cos \Delta\phi] \quad (4)$$

and t_r is the signal-to-reference transmission coefficient. Equation 4 indicates that several advantages can be obtained through the implementation of heterodyne detection. First, ISS signal magnitude can be increased by the attenuation factor (t_r), thereby achieving a high signal-to-noise ratio. Second, contributions from the amplitude and phase gratings can be decoupled by adjusting the relative phase $\Delta\phi$ between the signal and reference beams to be multiples of $\pi/2$. More precisely, through this phase adjustment, heterodyne detection produces a signal that varies with the material response parameters Δn or Δk and enables separation of the amplitude grating contribution from Δk and the phase grating contribution from Δn [145]. Additionally, subtracting experimental results between different $\Delta\phi$ can filter out unwanted signal components while remaining signal is doubled. Using this transient thermal grating approach, TGS provides information about thermoelastic properties of materials, such as thermal conductivity and elastic constants, through thermoelastic response measurements across various research fields, with specific applications detailed in a later section.

IV APPLICATIONS OF ISS

In ISS, surface acoustic waves (SAWs) are launched by a density grating from electrostriction or a thermal grating from optical absorption, depending on the nature of the medium. The wavelength of the excited SAW is determined by the optical grating period, enabling non-contact measurements of SAWs and guided modes in thin films, multilayers, liquids, and interfaces [146, 149, 151–155]. By measuring dispersion and velocities of surface acoustic modes, elastic moduli, film thickness, and depth profiling of structural defects can be obtained [53, 156, 157]. Figure 4(a) shows experimental results on stacked crystalline Si with polycrystalline Cu-Ta thin film layers, where the lowest acoustic mode was observed to exhibit a negative group velocity at a frequency near 190 MHz, analogous to Lamb modes in free plates [148]. ISS can also provide access to interfacial acoustics; for instance, co-propagating surface modes and a short-lived, high-velocity interfacial mode were observed at TiO₂-water interfaces [158], whereas at solid and glass-forming liquid interfaces, it has been applied to capture structural relaxation dynamics during the glass transition [159]. An-

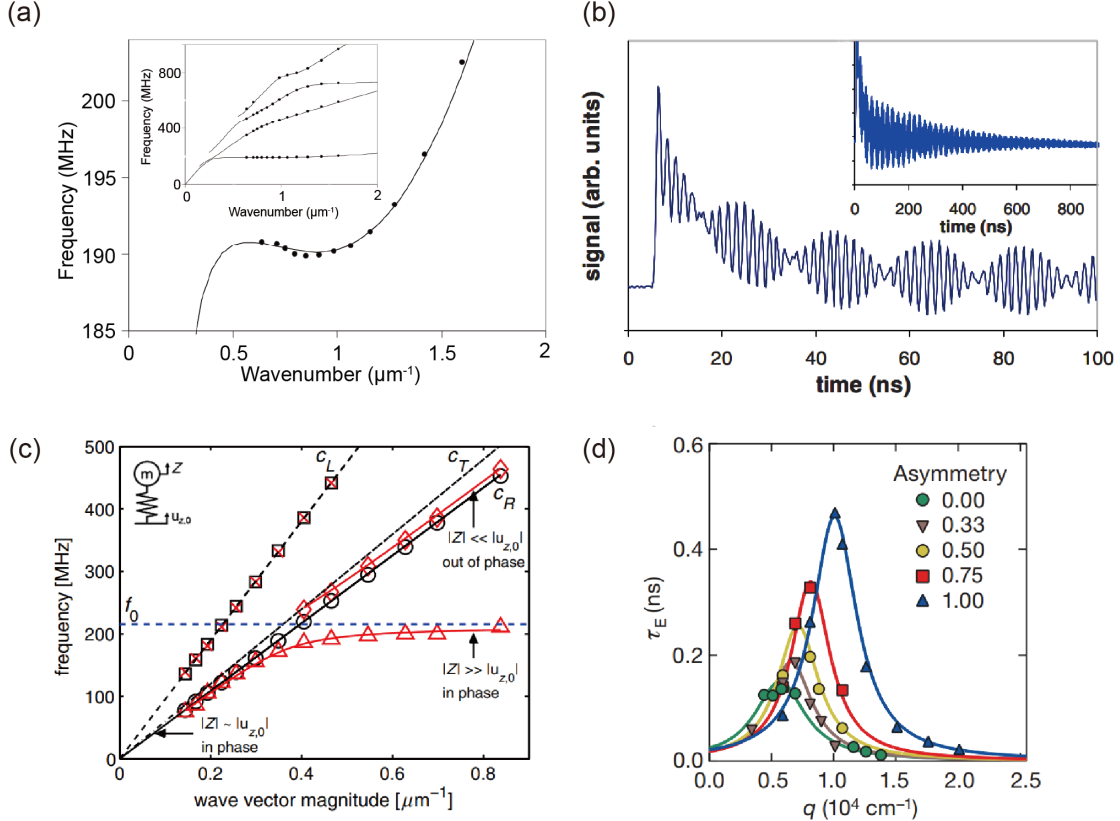


FIG. 4. (a) Measured (solid circles) and calculated (line) dispersion relation of the lowest frequency surface acoustic mode in a silicon thin film (Inset: dispersion curves of the four lowest frequency modes) [148]. Reprinted from A. A. Maznev et al. Appl. Phys. Lett. 95, 011903 (2009), with the permission of AIP Publishing. (b) TGS signal from a micro-patterned 1D phononic structure, showing acoustic oscillations associated with non-leaky, long-lived surface acoustic modes. (Inset: the same signal over a longer time scale) [149]. Reprinted from A. A. Maznev et al. J. Appl. Phys. 105, 123530 (2009), with the permission of AIP Publishing. (c) Acoustic dispersion of a 2D granular crystal, where red and black markers represent the measured frequencies with and without silica microspheres, respectively. A horizontal dotted line indicates the resonance frequency arising from microsphere-substrate adhesion [150]. Reprinted figure with permission from N. Boechler et al. Interaction of a Contact Resonance of Microspheres with Surface Acoustic Waves, Phys. Rev. Lett. 111, 036103 (2013). Copyright 2013 by the American Physical Society. (d) Measured spin helix lifetimes versus wavevector in GaAs/AlGaAs quantum wells, showing enhanced lifetime peaks to higher wavevectors with increasing doping asymmetry [62]. Reproduced with permission from J. D. Koralek et al. Emergence of the persistent spin helix in semiconductor quantum wells, Nature 458, 7238 (2009). Copyright 2009 Springer Nature.

other application of ISS includes probing the quality of adhesion and mechanical properties of coatings, such as MnO_2 films, where SAW velocity dispersion and Scholte wave velocities were measured to estimate Young's modulus and porosity of coatings [160].

ISS has also been employed to measure attenuation and dispersion relations of SAWs in phononic systems. In Fig. 4(b), a micro-patterned $\text{SiO}_2\text{-Si}$ structure exhibits TGS signal from spatially localized, non-leaky surface acoustic modes with lifetimes of hundreds of nanoseconds [149]. On the other hand, grooved silica substrate showed additional band gaps and leaky SAW modes [161]. In locally resonant acoustic metamaterials, hybridized flexural Lamb waves [56] and avoided crossings between contact resonances and Rayleigh modes, shown in Fig. 4(c), were observed [150, 162, 163]. More recently, ISS has moved from point spectroscopy to Brillouin microscopy of micromechanics in transparent and soft materials [54, 164–166]. Recent work has demonstrated rapid elastography with sub-millisecond acquisition time, enabling 2D Brillouin shift mapping of PDMS–methanol mixture with reduced photodamage [165].

By adjusting pump beams to be cross-polarized, transient spin grating spectroscopy can be realized, which is used to probe spin dynamics of electrons and excitons, and valley polarization dynamics across various semiconductors and magnetic materials, including low-dimensional systems such as quantum wells and quantum dots [63, 167–177]. Early seminal work using transient spin grating demonstrated that electron drift mobility and diffusion in $\text{GaAs}/\text{AlGaAs}$ multiple quantum wells can be measured via exploiting 90° polarization-rotation of a linearly polarized probe beam diffracted from spin grating, which isolates electron spin transport from ambipolar charge transport [178]. Wavevector-resolved spin grating subsequently revealed non-diffusive spin-polarization transport in semiconductor quantum wells, with the maximum spin decay time at a finite wavevector that contradicts predictions from simple diffusion theory due to spin-orbit coupling [179]. In addition, spin Coulomb drag effect in a two-dimensional electron gas was demonstrated using spin gratings, where electron-electron scattering transfers momentum between up- and down-spin channels, thereby suppressing macroscopic spin transport [61]. As shown in Fig. 4(d), spin gratings have been used to probe the tunability of spin polarization lifetimes; by varying the level of doping asymmetry to manipulate the strength of Rashba spin-orbit interaction, it was demonstrated that the peak lifetimes of persistent spin helix modes in $\text{GaAs}/\text{AlGaAs}$ quantum wells can be progressively shifted along wavevector [62]. More recently, TGS has been extensively

used to probe valley polarization dynamics in low-dimensional materials lacking inversion symmetry [63, 180, 181], including the observation of fluence-dependent valley decay rate in monolayer MoSe₂, where strong exciton-exciton interactions lead to fast valley depolarization lifetimes of a few picoseconds [63]. Together, these studies highlight the functionality of TGS for probing spin and valley transport across systems from bulk crystals to emerging quantum materials, providing insights into spin-orbit coupling and valley excitons that are essential for developing spintronic, valleytronic, and optoelectronic devices.

To extract thermal properties, thermal signals from ISTS measurements, also known as transient thermal grating, have been analyzed. For materials where the optical penetration depth exceeds the sample thickness, the heat transfer can be treated as pure one-dimensional. As a result, the thermal gratings with period L exponentially decay with an average decay time constant $\tau = 1/(\alpha q^2)$ in which α is in-plane thermal diffusivity and $q = 2\pi/L$ is the grating wavevector. This relation suggests that determining the thermal decay time constant at a given grating period enables measurement of the thermal diffusivity from which one can also calculate the thermal conductivity using the heat capacity. Figure 5(a) shows representative ISTS thermal decay signals measured in silicon thin film (thickness: 400 nm) [50] at various grating periods ranging from 3.2 to 18 μm . The signals consist of two components: an initial rise that quickly decays after the photoexcitation, followed by slower thermal decay with a time constant of few tens of nanoseconds. The first signal component is due to ambipolar diffusion, while the second component corresponds to the thermal decay signal. For silicon, the ambipolar diffusion coefficient is larger by an order of magnitude, compared with the thermal diffusivity [139, 183]. Therefore, electronic and thermal relaxation dynamics can be distinctly resolved in the time domain. The decay time increases with the grating period and the decay rate $\gamma = 1/\tau$ is related to q^2 by a linear trend at sufficiently large grating period as shown in Fig. 5(b). Here, the corresponding thermal conductivity at large grating period is the bulk value. However, as the grating period decreases, γ versus q^2 deviates from the linear trend and the actual thermal decay becomes slower compared to the prediction from the heat diffusion theory. It has been established that the deviation is due to ballistic transport of thermal acoustic vibrations over the grating period.

At the onset of ballistic phonon transport, the thermal conductivity contribution from heat-carrying, thermal phonons with MFP (Λ) longer than the thermal length starts to de-

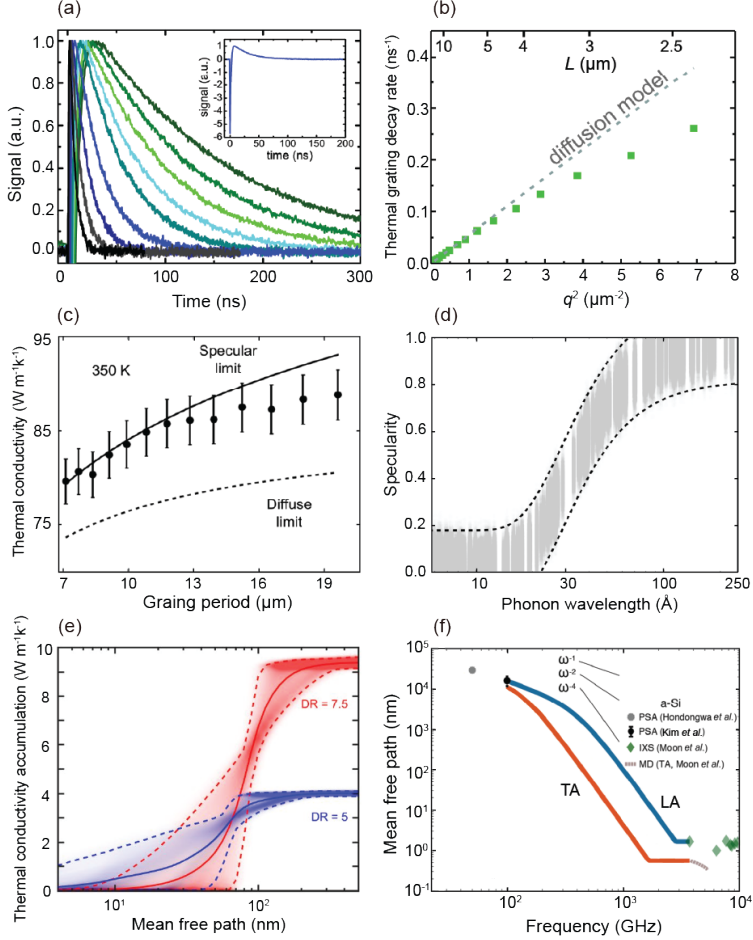


FIG. 5. (a) Thermal decay signals of silicon at several transient grating periods. The inset shows the complete wave form for a representative grating period of $7.5 \mu\text{m}$. The thermal signal decays slower as the grating period increases. Reprinted figure with permission from Johnson *et al.*, Phys. Rev. Lett., **110**, 025901 2013. Copyright 2013 by the American Physical Society [50]. (b) Thermal decay rate versus grating wavevector squared, q^2 [50]. As grating period decreases, the thermal decay rate deviates from what is predicted from heat diffusion theory. (c) Measured thermal conductivity versus grating period at 350 K in silicon thin film. As grating period decreases, the measured thermal conductivity approaches specular limit [182]. (d) Reconstructed phonon specularity versus phonon wavelength from grating period dependent thermal conductivity measurements including (c). As wavelength of phonon gets larger, specularity increases [182]. (e) Reconstructed thermal conductivity accumulation of partially ordered polyethylene thin films [57]. (f) Reconstructed frequency dependent MFPs of thermal acoustic excitations in aSi. Reprinted figure with permission from Kim *et al.*, Phys. Rev. Materials, **5**, 065602 2021. Copyright 2021 by the American Physical Society [58].

crease [184]. The corresponding grating period dependent thermal conductivity is expressed as [185]

$$\kappa(q) = \int_0^\infty S(x)f(\Lambda_\omega) d\Lambda_\omega = \int_0^\infty qK(x)F(\Lambda_\omega) d\Lambda_\omega \quad (5)$$

where $x = q\Lambda_\omega$, and $K(x) = -dS/dx$ with $S(x)$ being the heat suppression function that accounts for effective heat flux, which is reduced compared to Fourier law predicted heat flux due to quasi-ballistic transport [185]. The cumulative thermal conductivity, $F(\Lambda_\omega)(= \int_0^{\Lambda_\omega} f(\Lambda)d\Lambda)$, provides insight into microscopic heat conduction properties by enabling to examine the contributions of MFPs of heat carriers to the thermal conductivity. By changing the integration variable from MFP to frequency [186], one can also express Eq. 5 as

$$\kappa(q) = \sum_{\mathbf{p}} \int_0^\infty S(x_{\mathbf{p}}) [C_{\mathbf{p}}(\omega)v_{\mathbf{p}}(\omega)\Lambda_{\mathbf{p}}(\omega)] d\omega \quad (6)$$

where \mathbf{p} indexes the polarization and $C_{\mathbf{p}}$ and $v_{\mathbf{p}}$ are the specific heat and group velocity of thermal energy carriers. In Eq. 6, $\Lambda_{\mathbf{p}}(\omega)$ is MFPs versus frequency, representing scattering mechanisms that depend on the frequency. In TGS, it has been established that the cumulative thermal conductivity and the frequency versus MFPs can be reconstructed by solving Eqs. 5 and 6, and that ill-posed problems of Eqs. 5 and 6 can be solved using numerical optimizations or statistical methods [57, 182, 185].

The measurements of the grating period thermal conductivity in macroscopic thin films have provided insights into the understanding of microscopic transport properties governing heat conduction along the in-plane direction. While it has been recognized that atomic scale imperfections such as surface roughness strongly affects phonon boundary scattering, hence the effective thermal resistance, experimentally resolving the boundary conditions at which phonon specular reflections occur has been challenging [187]. Ravichandran *et al.* have demonstrated a metrology to extract specular parameters from the ISTS measurements on crystalline silicon thin films, as shown in Fig. 5(c) [182]. The experimentally resolved specularity is shown in Fig. 5(d), in which the spectral dependence of phonon reflections at the boundary can be seen.

Additionally, ISTS measurements on thermally conductive polymers [57, 188] have revealed microscopic transport properties that lead to exceptional thermal conductivities. It has been shown that the thermal conductivities of structurally-engineered semi-crystalline polymers including polyethylene (PE) can achieve orders of magnitude increases, which

can be as high as those in many condensed matters. While such thermal conductivity enhancements have been typically interpreted using effective medium models [189–191], debate has existed concerning the origin of the high thermal conductivity, particularly for highly oriented polymers [192, 193]. Recent ISTS measurements applied to stretched PEs have provided insights into microscopic origins that lead to high thermal conductivities in these specimens. As shown in Fig. 5(e), for partially oriented PEs, it has been shown that MFP of phonons that substantially contribute to the heat conduction is on the order of 100 nm, which exceeds the grain size of ~ 60 nm, indicating ballistic propagation of phonons across the grain boundaries [57]. Additionally, more recent measurements on highly oriented PEs have shown that thermal conductivity of macroscopic thin films of PE can be as high as $\sim 50 \text{ Wm}^{-1}\text{K}^{-1}$, which was primarily attributed to thermal acoustic phonons that propagate over a few hundreds nanometers, limited by enlarged crystals in them [188].

ISTS experiments have also been applied to amorphous solids and experimentally probed the scattering of thermal vibrations that occurs distinctly in them, which was not captured using prior numerical studies [58]. An experimental approach that enables to reconstruct the frequency dependent MFPs along with MFP accumulation function by utilizing constraints were demonstrated and applied to amorphous silicon (aSi). Results are shown in Fig 5(f), in which power-law dependence of MFPs ($\Lambda \sim \omega^{-n}$) can be seen, indicating the characteristics of scattering that depends on the frequency. In particular, Rayleigh-type scattering as a primary scattering mechanism ($n = 4$) was observed above 1 THz for aSi, which contradicts with predictions from prior normal mode analysis yet agrees with experimental results in other glassy substances such as vitreous silica.

V OUTLOOK AND CONCLUSION

To make further developments in Brillouin scattering, recent efforts have focused on pushing the limits of the spatiotemporal resolution of the technique. The introduction of short wavelength light sources in TGS setups has enabled grating periods approaching sub-micrometer length scales, allowing researchers to probe non-diffusive dynamics in materials. Free electron lasers in the extreme ultraviolet (EUV) [194–196] and X-ray [197] bands have been implemented to further increase penetration depth and push grating period limits below nanometer scales. These grating periods can elucidate magnetic dynamics

and unconventional heat transport at nanometer scales. In the time domain, fast electronic processes such as electron-hole recombination can be temporally resolved with attosecond-scale temporal resolution by implementing both sub-femtosecond excitation and detection processes [198, 199], providing valuable insights into fast electronic processes such as carrier thermalization and recombination processes. Furthermore, when combined with enhanced temporal and spatial resolution, spin gratings also have potential for studying electronic spin transport dynamics that can establish the theoretical background for spintronic device applications.

Brillouin scattering has also expanded into applications beyond materials science, including optical communications and biological imaging. In photonics, stimulated Brillouin processes have been investigated to exploit enhanced Brillouin gain in optical fibers and waveguides for applications in microwave photonics and signal processing [200–202]. This enables ultra-low-loss on-chip platforms that provide narrowband optical gain, demonstrating the feasibility of integrated Brillouin photonics [203, 204]. In the field of life sciences, Brillouin microscopy has emerged as one of the instrumental techniques for mapping mechanical properties of soft and liquid biological samples. A pioneering work reported the first *in situ* three-dimensional imaging of the intraocular lens of a mouse using confocal Brillouin microscopy [205]. Since then, Brillouin technique has been applied to diverse biological systems, including 3D imaging of human cornea both *in vivo* [206] and *ex vivo* [207], probing intracellular stress granule mechanics during liquid-to-solid phase transition [208], and mapping intracellular biomechanics within a whole living organism [209]. These advances highlight the possible translation of Brillouin microscopy from basic research to clinical diagnostics, particularly in ophthalmology [210–212].

To conclude, Brillouin scattering spectroscopy remains an indispensable technique for probing low-frequency acoustic and spin waves in thin films and bulk materials. By providing access to these sub-THz excitations, it provides information on dispersions and lifetimes of these quasiparticles for understanding energy transport in novel materials. By integrating with other foundational inelastic scattering techniques, such as Raman spectroscopy, INS, and IXS, Brillouin scattering spectroscopy can bridge the gap in length and time scales of energy transport processes that were previously inaccessible. This provides a quantitative experimental platform to gain insight into nanoscale energy transport and conversion processes, with direct implications for guiding the design of thermoelectrics, thermal interface

materials, and nanostructured systems for energy harvesting, thermal management, and microelectronics.

ACKNOWLEDGEMENTS

This work was supported by the National Research Foundation of Korea (NRF) grant funded by the Korea government(MSIT)(No. RS-2023-00211070 and No. RS-2024-00403173).

AUTHOR CONTRIBUTIONS

Hyemin Kim: Writing - original draft (equal); Writing - review & editing (equal).
Hyungseok Kim: Writing - original draft (equal); Writing - review & editing (equal). Taeyong Kim: Conceptualization (lead); Funding acquisition (lead); Supervision (lead); Writing - original draft (supporting); Writing - review & editing (equal).

DATA AVAILABILITY

Data sharing is not applicable to this article as no new data were created or analyzed in this study.

COMPETING INTERESTS

The authors have no conflicts to disclose.

REFERENCES

- [1] Gang Chen. *Nanoscale Energy Transport And Conversion: A Parallel Treatment Of Electrons, Molecules, Phonons, And Photons*. Oxford University Press, 03 2005. ISBN 9780195159424. doi:10.1093/oso/9780195159424.001.0001. URL <https://doi.org/10.1093/oso/9780195159424.001.0001>.
- [2] Eric Pop. Energy dissipation and transport in nanoscale devices. *Nano Research*, 3(3):147–169, Mar 2010. ISSN 1998-0000. doi:10.1007/s12274-010-1019-z. URL <https://doi.org/10.1007/s12274-010-1019-z>.
- [3] John T. Gaskins, Patrick E. Hopkins, Devin R. Merrill, Sage R. Bauers, Erik Hadland, David C. Johnson, Donghyi Koh, Jung Hwan Yum, Sanjay Banerjee, Bradley J. Nordell,

- Michelle M. Paquette, Anthony N. Caruso, William A. Lanford, Patrick Henry, Liza Ross, Han Li, Liyi Li, Marc French, Antonio M. Rudolph, and Sean W. King. Review—investigation and review of the thermal, mechanical, electrical, optical, and structural properties of atomic layer deposited high-k dielectrics: Beryllium oxide, aluminum oxide, hafnium oxide, and aluminum nitride. *ECS Journal of Solid State Science and Technology*, 6(10):N189, oct 2017. doi:10.1149/2.0091710jss. URL <https://dx.doi.org/10.1149/2.0091710jss>.
- [4] Ethan A. Scott, John T. Gaskins, Sean W. King, and Patrick E. Hopkins. Thermal conductivity and thermal boundary resistance of atomic layer deposited high-k dielectric aluminum oxide, hafnium oxide, and titanium oxide thin films on silicon. *APL Materials*, 6(5):058302, 05 2018. ISSN 2166-532X. doi:10.1063/1.5021044. URL <https://doi.org/10.1063/1.5021044>.
 - [5] Ali Shakouri. Recent developments in semiconductor thermoelectric physics and materials. *Annual Review of Materials Research*, 41(Volume 41, 2011):399–431, 2011. ISSN 1545-4118. doi:<https://doi.org/10.1146/annurev-matsci-062910-100445>. URL <https://www.annualreviews.org/content/journals/10.1146/annurev-matsci-062910-100445>.
 - [6] Madhubanti Mukherjee, Ashutosh Srivastava, and Abhishek K. Singh. Recent advances in designing thermoelectric materials. *J. Mater. Chem. C*, 10:12524–12555, 2022. doi: 10.1039/D2TC02448A. URL <http://dx.doi.org/10.1039/D2TC02448A>.
 - [7] Qihao Zhang, Kangfa Deng, Lennart Wilkens, Heiko Reith, and Kornelius Nielsch. Microthermoelectric devices. *Nature Electronics*, 5(6):333–347, Jun 2022. ISSN 2520-1131. doi: 10.1038/s41928-022-00776-0. URL <https://doi.org/10.1038/s41928-022-00776-0>.
 - [8] David G. Cahill, Wayne K. Ford, Kenneth E. Goodson, Gerald D. Mahan, Arun Majumdar, Humphrey J. Maris, Roberto Merlin, and Simon R. Phillpot. Nanoscale thermal transport. *Journal of Applied Physics*, 93(2):793–818, 01 2003. ISSN 0021-8979. doi:10.1063/1.1524305. URL <https://doi.org/10.1063/1.1524305>.
 - [9] David G. Cahill, Paul V. Braun, Gang Chen, David R. Clarke, Shanhui Fan, Kenneth E. Goodson, Paweł Kebinski, William P. King, Gerald D. Mahan, Arun Majumdar, Humphrey J. Maris, Simon R. Phillpot, Eric Pop, and Li Shi. Nanoscale thermal transport. ii. 2003–2012. *Applied Physics Reviews*, 1(1):011305, 01 2014. ISSN 1931-9401. doi: 10.1063/1.4832615. URL <https://doi.org/10.1063/1.4832615>.
 - [10] O. Delaire, J. Ma, K. Marty, A. F. May, M. A. McGuire, M.-H. Du, D. J. Singh, A. Podlesnyak, G. Ehlers, M. D. Lumsden, and B. C. Sales. Giant anharmonic phonon scattering in pbte.

Nature Materials, 10(8):614–619, Aug 2011. ISSN 1476-4660. doi:10.1038/nmat3035. URL <https://doi.org/10.1038/nmat3035>.

- [11] A. C. Ferreira, A. Létoublon, S. Paofai, S. Raymond, C. Ecolivet, B. Rufflé, S. Cordier, C. Katan, M. I. Saidaminov, A. A. Zhumekenov, O. M. Bakr, J. Even, and P. Bourges. Elastic softness of hybrid lead halide perovskites. *Phys. Rev. Lett.*, 121:085502, Aug 2018. doi:10.1103/PhysRevLett.121.085502. URL <https://link.aps.org/doi/10.1103/PhysRevLett.121.085502>.
- [12] C. Masciovecchio, G. Ruocco, F. Sette, P. Benassi, A. Cunsolo, M. Krisch, V. Mazzacurati, A. Mermet, G. Monaco, and R. Verbeni. High-frequency propagating modes in vitreous silica at 295 k. *Phys. Rev. B*, 55:8049–8051, Apr 1997. doi:10.1103/PhysRevB.55.8049. URL <https://link.aps.org/doi/10.1103/PhysRevB.55.8049>.
- [13] G. Baldi, V. M. Giordano, G. Monaco, and B. Ruta. Sound attenuation at terahertz frequencies and the boson peak of vitreous silica. *Phys. Rev. Lett.*, 104:195501, May 2010. doi:10.1103/PhysRevLett.104.195501. URL <https://link.aps.org/doi/10.1103/PhysRevLett.104.195501>.
- [14] Francesco Sette, Michael H. Krisch, Claudio Masciovecchio, Giancarlo Ruocco, and Giulio Monaco. Dynamics of glasses and glass-forming liquids studied by inelastic x-ray scattering. *Science*, 280(5369):1550–1555, 1998. doi:10.1126/science.280.5369.1550. URL <https://www.science.org/doi/abs/10.1126/science.280.5369.1550>.
- [15] Paula M. B. Piccoli, Thomas F. Koetzle, and Arthur J. Schultz. Single crystal neutron diffraction for the inorganic chemist – a practical guide. *Comments on Inorganic Chemistry*, 28(1-2):3–38, 2007. doi:10.1080/02603590701394741. URL <https://doi.org/10.1080/02603590701394741>.
- [16] A. Wischnewski, U. Buchenau, A. J. Dianoux, W. A. Kamitakahara, and J. L. Zarestky. Sound-wave scattering in silica. *Phys. Rev. B*, 57:2663–2666, Feb 1998. doi:10.1103/PhysRevB.57.2663. URL <https://link.aps.org/doi/10.1103/PhysRevB.57.2663>.
- [17] G. Baldi, V.M. Giordano, G. Monaco, and B. Ruta. High frequency acoustic attenuation of vitreous silica: New insight from inelastic x-ray scattering. *Journal of Non-Crystalline Solids*, 357(2):538–541, 2011. ISSN 0022-3093. doi:<https://doi.org/10.1016/j.jnoncrysol.2010.05.085>. URL <https://www.sciencedirect.com/science/article/pii/S0022309310004849>. 6th

International Discussion Meeting on Relaxation in Complex Systems.

- [18] Willes H Weber and Roberto Merlin. *Raman scattering in materials science*, volume 42. Springer Science & Business Media, 2013.
- [19] Fariborz Kargar and Alexander A. Balandin. Advances in brillouin–mandelstam light-scattering spectroscopy. *Nature Photonics*, 15(10):720–731, Oct 2021. ISSN 1749-4893. doi: 10.1038/s41566-021-00836-5. URL <https://doi.org/10.1038/s41566-021-00836-5>.
- [20] Léon Brillouin. Diffusion de la lumière et des rayons x par un corps transparent homogène - influence de l'agitation thermique. *Ann. Phys.*, 9(17):88–122, 1922. doi: 10.1051/anphys/192209170088. URL <https://doi.org/10.1051/anphys/192209170088>.
- [21] Leonid Issaakovitch Mandelstam. Light scattering by inhomogeneous media. *Zh. Russ. Fiz. Khim. Ova*, 58(381):146, 1926.
- [22] E. Gross. Change of wave-length of light due to elastic heat waves at scattering in liquids. *Nature*, 126(3171):201–202, Aug 1930. ISSN 1476-4687. doi:10.1038/126201a0. URL <https://doi.org/10.1038/126201a0>.
- [23] E. Gross. The splitting of spectral lines at scattering of light by liquids. *Nature*, 126(3176): 400–400, Sep 1930. ISSN 1476-4687. doi:10.1038/126400a0. URL <https://doi.org/10.1038/126400a0>.
- [24] J.R. Sandercock. Light scattering from surface acoustic phonons in metals and semiconductors. *Solid State Communications*, 26(8):547–551, 1978. ISSN 0038-1098. doi: [https://doi.org/10.1016/0038-1098\(78\)91307-8](https://doi.org/10.1016/0038-1098(78)91307-8). URL <https://www.sciencedirect.com/science/article/pii/0038109878913078>.
- [25] R. Y. Chiao, C. H. Townes, and B. P. Stoicheff. Stimulated brillouin scattering and coherent generation of intense hypersonic waves. *Phys. Rev. Lett.*, 12:592–595, May 1964. doi: 10.1103/PhysRevLett.12.592. URL <https://link.aps.org/doi/10.1103/PhysRevLett.12.592>.
- [26] M. J. Damzen, V. Vlad, Anca Mocofanescu, and V. Babin. *Stimulated Brillouin scattering: fundamentals and applications*. CRC press, 2003.
- [27] Robert W Boyd, Alexander L Gaeta, and Enno Giese. *Nonlinear optics*. Springer, 2008.
- [28] Benjamin J. Eggleton, Christopher G. Poulton, Peter T. Rakich, Michael. J. Steel, and Gaurav Bahl. Brillouin integrated photonics. *Nature Photonics*, 13(10):664–677, Oct 2019. ISSN 1749-4893. doi:10.1038/s41566-019-0498-z. URL <https://doi.org/10.1038/s41566-019-0498-z>.

- [29] Yong-Xin Yan, Jr. Gamble, Edward B., and Keith A. Nelson. Impulsive stimulated scattering: General importance in femtosecond laser pulse interactions with matter, and spectroscopic applications. *The Journal of Chemical Physics*, 83(11):5391–5399, 12 1985. ISSN 0021-9606. doi:10.1063/1.449708. URL <https://doi.org/10.1063/1.449708>.
- [30] Yong-Xin Yan and Keith A. Nelson. Impulsive stimulated light scattering. i. general theory. *The Journal of Chemical Physics*, 87(11):6240–6256, 12 1987. ISSN 0021-9606. doi:10.1063/1.453733. URL <https://doi.org/10.1063/1.453733>.
- [31] H Boersch and H Eichler. Beugung an einem mit stehenden lichtwellen gepumpten rubin. *Zeitschrift für Angewandte Physik*, 22(5):378, 1967.
- [32] Antoine Létoublon, Serge Paofai, Benoît Rufflé, Philippe Bourges, Bernard Hehlen, Thierry Michel, Claude Ecolivet, Olivier Durand, Stéphane Cordier, Claudine Katan, and Jacky Even. Elastic Constants, Optical Phonons, and Molecular Relaxations in the High Temperature Plastic Phase of the $\text{CH}_3\text{NH}_3\text{PbBr}_3$ Hybrid Perovskite. *The Journal of Physical Chemistry Letters*, 7(19):3776–3784, 2016. doi:10.1021/acs.jpclett.6b01709. URL <https://doi.org/10.1021/acs.jpclett.6b01709>. PMID: 27601100.
- [33] Ho-Kwang Mao, Xiao-Jia Chen, Yang Ding, Bing Li, and Lin Wang. Solids, liquids, and gases under high pressure. *Rev. Mod. Phys.*, 90:015007, Mar 2018. doi:10.1103/RevModPhys.90.015007. URL <https://link.aps.org/doi/10.1103/RevModPhys.90.015007>.
- [34] John Sandercock. Some recent applications of brillouin scattering in solid state physics. In H. J. Queisser, editor, *Festkörperprobleme 15: Plenary Lectures of the Divisions “Semiconductor Physics”, “Low Temperature Physics”, “Metal Physics” of the German Physical Society Münster, March 17–21, 1975*, pages 183–202. Springer Berlin Heidelberg, Berlin, Heidelberg, 1975. ISBN 978-3-540-75347-6. doi:10.1007/BFb0107378. URL <https://doi.org/10.1007/BFb0107378>.
- [35] Jae-Hyeon Ko, Tae Hyun Kim, K. Roleder, D. Rytz, and Seiji Kojima. Precursor dynamics in the ferroelectric phase transition of barium titanate single crystals studied by brillouin light scattering. *Phys. Rev. B*, 84:094123, Sep 2011. doi:10.1103/PhysRevB.84.094123. URL <https://link.aps.org/doi/10.1103/PhysRevB.84.094123>.
- [36] G. Benedek and T. Greystak. Brillouin scattering in liquids. *Proceedings of the IEEE*, 53(10):1623–1629, 1965. doi:10.1109/PROC.1965.4271.

- [37] Fariborz Kargar, Bishwajit Debnath, Joona-Pekko Kakko, Antti Säynätjoki, Harri Lipsanen, Denis L. Nika, Roger K. Lake, and Alexander A. Balandin. Direct observation of confined acoustic phonon polarization branches in free-standing semiconductor nanowires. *Nature Communications*, 7(1):13400, Nov 2016. ISSN 2041-1723. doi:10.1038/ncomms13400. URL <https://doi.org/10.1038/ncomms13400>.
- [38] O. Florez, G. Arregui, M. Albrechtsen, R. C. Ng, J. Gomis-Bresco, S. Stobbe, C. M. Sotomayor-Torres, and P. D. García. Engineering nanoscale hypersonic phonon transport. *Nature Nanotechnology*, 17(9):947–951, Sep 2022. ISSN 1748-3395. doi:10.1038/s41565-022-01178-1. URL <https://doi.org/10.1038/s41565-022-01178-1>.
- [39] V. E. Demidov, J. Jersch, K. Rott, P. Krzysteczko, G. Reiss, and S. O. Demokritov. Non-linear propagation of spin waves in microscopic magnetic stripes. *Phys. Rev. Lett.*, 102: 177207, Apr 2009. doi:10.1103/PhysRevLett.102.177207. URL <https://link.aps.org/doi/10.1103/PhysRevLett.102.177207>.
- [40] K. Vogt, F. Y. Fradin, J. E. Pearson, T. Sebastian, S. D. Bader, B. Hillebrands, A. Hoffmann, and H. Schultheiss. Realization of a spin-wave multiplexer. *Nature Communications*, 5(1): 3727, Apr 2014. ISSN 2041-1723. doi:10.1038/ncomms4727. URL <https://doi.org/10.1038/ncomms4727>.
- [41] Hans T. Nembach, Justin M. Shaw, Mathias Weiler, Emilie Jué, and Thomas J. Silva. Linear relation between heisenberg exchange and interfacial dzyaloshinskii-moriya interaction in metal films. *Nature Physics*, 11(10):825–829, Oct 2015. ISSN 1745-2481. doi: 10.1038/nphys3418. URL <https://doi.org/10.1038/nphys3418>.
- [42] J. Holanda, D. S. Maior, A. Azevedo, and S. M. Rezende. Detecting the phonon spin in magnon–phonon conversion experiments. *Nature Physics*, 14(5):500–506, May 2018. ISSN 1745-2481. doi:10.1038/s41567-018-0079-y. URL <https://doi.org/10.1038/s41567-018-0079-y>.
- [43] Vladislav E. Demidov, Sergei Urazhdin, Ronghua Liu, Boris Divinskiy, Andrey Telegin, and Sergej O. Demokritov. Excitation of coherent propagating spin waves by pure spin currents. *Nature Communications*, 7(1):10446, Jan 2016. ISSN 2041-1723. doi:10.1038/ncomms10446. URL <https://doi.org/10.1038/ncomms10446>.
- [44] Vladislav E. Demidov, Sergej O. Demokritov, Karsten Rott, Patryk Krzysteczko, and Guenter Reiss. Self-focusing of spin waves in permalloy microstripes. *Applied Physics Letters*, 91(25):

252504, 12 2007. ISSN 0003-6951. doi:10.1063/1.2825421. URL <https://doi.org/10.1063/1.2825421>.

- [45] K. Vogt, H. Schultheiss, S. Jain, J. E. Pearson, A. Hoffmann, S. D. Bader, and B. Hillebrands. Spin waves turning a corner. *Applied Physics Letters*, 101(4):042410, 07 2012. ISSN 0003-6951. doi:10.1063/1.4738887. URL <https://doi.org/10.1063/1.4738887>.
- [46] Jaehun Cho, Nam-Hui Kim, Sukmock Lee, June-Seo Kim, Reinoud Lavrijsen, Aurelie Solignac, Yuxiang Yin, Dong-Soo Han, Niels J. J. van Hoof, Henk J. M. Swagten, Bert Koopmans, and Chun-Yeol You. Thickness dependence of the interfacial dzyaloshinskii–moriya interaction in inversion symmetry broken systems. *Nature Communications*, 6(1):7635, Jul 2015. ISSN 2041-1723. doi:10.1038/ncomms8635. URL <https://doi.org/10.1038/ncomms8635>.
- [47] S. O. Demokritov, V. E. Demidov, O. Dzyapko, G. A. Melkov, A. A. Serga, B. Hillebrands, and A. N. Slavin. Bose–einstein condensation of quasi-equilibrium magnons at room temperature under pumping. *Nature*, 443(7110):430–433, Sep 2006. ISSN 1476-4687. doi:10.1038/nature05117. URL <https://doi.org/10.1038/nature05117>.
- [48] I. V. Borisenko, B. Divinskiy, V. E. Demidov, G. Li, T. Nattermann, V. L. Pokrovsky, and S. O. Demokritov. Direct evidence of spatial stability of bose-einstein condensate of magnons. *Nature Communications*, 11(1):1691, Apr 2020. ISSN 2041-1723. doi:10.1038/s41467-020-15468-6. URL <https://doi.org/10.1038/s41467-020-15468-6>.
- [49] Jeremy A. Johnson, Alexei A. Maznev, Mayank T. Bulsara, Eugene A. Fitzgerald, T. C. Harman, S. Calawa, C. J. Vineis, G. Turner, and Keith A. Nelson. Phase-controlled, heterodyne laser-induced transient grating measurements of thermal transport properties in opaque material. *Journal of Applied Physics*, 111(2):023503, 01 2012. ISSN 0021-8979. doi:10.1063/1.3675467. URL <https://doi.org/10.1063/1.3675467>.
- [50] Jeremy A. Johnson, A. A. Maznev, John Cuffe, Jeffrey K. Eliason, Austin J. Minnich, Timothy Kehoe, Clivia M. Sotomayor Torres, Gang Chen, and Keith A. Nelson. Direct measurement of room-temperature nondiffusive thermal transport over micron distances in a silicon membrane. *Phys. Rev. Lett.*, 110:025901, Jan 2013. doi:10.1103/PhysRevLett.110.025901. URL <https://link.aps.org/doi/10.1103/PhysRevLett.110.025901>.
- [51] John Cuffe, Jeffrey K. Eliason, A. A. Maznev, Kimberlee C. Collins, Jeremy A. Johnson, Andrey Shchepetov, Mika Prunnila, Jouni Ahopelto, Clivia M. Sotomayor Torres, Gang Chen, and Keith A. Nelson. Reconstructing phonon mean-free-path contributions to ther-

- mal conductivity using nanoscale membranes. *Phys. Rev. B*, 91:245423, Jun 2015. doi: 10.1103/PhysRevB.91.245423. URL <https://link.aps.org/doi/10.1103/PhysRevB.91.245423>.
- [52] Chen Li, Hao Ma, Tianyang Li, Jinghang Dai, Md. Abu Jafar Rasel, Alessandro Mattoni, Ahmet Alatas, Malcolm G. Thomas, Zachary W. Rouse, Avi Shragai, Shefford P. Baker, B. J. Ramshaw, Joseph P. Feser, David B. Mitzi, and Zhiting Tian. Remarkably weak anisotropy in thermal conductivity of two-dimensional hybrid perovskite butylammonium lead iodide crystals. *Nano Letters*, 21(9):3708–3714, 2021. doi:10.1021/acs.nanolett.0c04550. URL <https://doi.org/10.1021/acs.nanolett.0c04550>. PMID: 33938755.
- [53] John A. Rogers, Alex A. Maznev, Matthew J. Banet, and Keith A. Nelson. Optical generation and characterization of acoustic waves in thin films: Fundamentals and applications. *Annual Review of Materials Research*, 30(Volume 30, 2000):117–157, 2000. ISSN 1545-4118. doi: <https://doi.org/10.1146/annurev.matsci.30.1.117>. URL <https://www.annualreviews.org/content/journals/10.1146/annurev.matsci.30.1.117>.
- [54] Benedikt Krug, Nektarios Koukourakis, and Juergen W. Czarske. Impulsive stimulated brillouin microscopy for non-contact, fast mechanical investigations of hydrogels. *Opt. Express*, 27(19):26910–26923, Sep 2019. doi:10.1364/OE.27.026910. URL <https://opg.optica.org/oe/abstract.cfm?URI=oe-27-19-26910>.
- [55] Tina Hecksher, Darius H. Torchinsky, Christoph Klieber, Jeremy A. Johnson, Jeppe C. Dyre, and Keith A. Nelson. Toward broadband mechanical spectroscopy. *Proceedings of the National Academy of Sciences*, 114(33):8710–8715, 2017. doi:10.1073/pnas.1707251114. URL <https://www.pnas.org/doi/abs/10.1073/pnas.1707251114>.
- [56] A. Khanolkar, S. Wallen, M. Abi Ghanem, J. Jenks, N. Vogel, and N. Boechler. A self-assembled metamaterial for lamb waves. *Applied Physics Letters*, 107(7):071903, 08 2015. ISSN 0003-6951. doi:10.1063/1.4928564. URL <https://doi.org/10.1063/1.4928564>.
- [57] Andrew B. Robbins, Stavros X. Drakopoulos, Ignacio Martin-Fabiani, Sara Ronca, and Austin J. Minnich. Ballistic thermal phonons traversing nanocrystalline domains in oriented polyethylene. *Proceedings of the National Academy of Sciences*, 116(35):17163–17168, 2019. doi:10.1073/pnas.1905492116. URL <https://www.pnas.org/doi/abs/10.1073/pnas.1905492116>.

- [58] Taeyong Kim, Jaeyun Moon, and Austin J. Minnich. Origin of micrometer-scale propagation lengths of heat-carrying acoustic excitations in amorphous silicon. *Phys. Rev. Mater.*, 5: 065602, Jun 2021. doi:10.1103/PhysRevMaterials.5.065602. URL <https://link.aps.org/doi/10.1103/PhysRevMaterials.5.065602>.
- [59] S. Huberman, R. A. Duncan, K. Chen, B. Song, V. Chiloyan, Z. Ding, A. A. Maznev, G. Chen, and K. A. Nelson. Observation of second sound in graphite at temperatures above 100 k. *Science*, 364(6438):375–379, 2019. doi:10.1126/science.aav3548. URL <https://www.science.org/doi/abs/10.1126/science.aav3548>.
- [60] Zhiwei Ding, Ke Chen, Bai Song, Jungwoo Shin, Alexei A. Maznev, Keith A. Nelson, and Gang Chen. Observation of second sound in graphite over 200 k. *Nature Communications*, 13(1):285, Jan 2022. ISSN 2041-1723. doi:10.1038/s41467-021-27907-z. URL <https://doi.org/10.1038/s41467-021-27907-z>.
- [61] C. P. Weber, N. Gedik, J. E. Moore, J. Orenstein, J. Stephens, and D. D. Awschalom. Observation of spin coulomb drag in a two-dimensional electron gas. *Nature*, 437(7063): 1330–1333, Oct 2005. ISSN 1476-4687. doi:10.1038/nature04206. URL <https://doi.org/10.1038/nature04206>.
- [62] J. D. Koralek, C. P. Weber, J. Orenstein, B. A. Bernevig, Shou-Cheng Zhang, S. Mack, and D. D. Awschalom. Emergence of the persistent spin helix in semiconductor quantum wells. *Nature*, 458(7238):610–613, Apr 2009. ISSN 1476-4687. doi:10.1038/nature07871. URL <https://doi.org/10.1038/nature07871>.
- [63] Fahad Mahmood, Zhanybek Alpichshev, Yi-Hsien Lee, Jing Kong, and Nuh Gedik. Observation of exciton–exciton interaction mediated valley depolarization in monolayer mose2. *Nano Letters*, 18(1):223–228, 2018. doi:10.1021/acs.nanolett.7b03953. URL <https://doi.org/10.1021/acs.nanolett.7b03953>. PMID: 29239177.
- [64] F. Bencivenga, F. Capotondi, L. Foglia, R. Mincigrucci, and C. Masciovecchio. Extreme ultraviolet transient gratings. *Advances in Physics: X*, 8(1):2220363, 2023. doi:10.1080/23746149.2023.2220363. URL <https://doi.org/10.1080/23746149.2023.2220363>.
- [65] C. Wolff, M. J. A. Smith, B. Stiller, and C. G. Poulton. Brillouin scattering—theory and experiment: tutorial. *J. Opt. Soc. Am. B*, 38(4):1243–1269, Apr 2021. doi:10.1364/JOSAB.416747. URL <https://opg.optica.org/josab/abstract.cfm?URI=josab-38-4-1243>.

- [66] G. B. Benedek and K. Fritsch. Brillouin scattering in cubic crystals. *Phys. Rev.*, 149:647–662, Sep 1966. doi:10.1103/PhysRev.149.647. URL <https://link.aps.org/doi/10.1103/PhysRev.149.647>.
- [67] Bruce J Berne and Robert Pecora. *Dynamic light scattering: with applications to chemistry, biology, and physics*. Courier Corporation, 2000.
- [68] S. Shapiro, M. McClintock, D. Jennings, and R. Barger. Brillouin scattering in liquids at 4880Å. *IEEE Journal of Quantum Electronics*, 2(5):89–93, 1966. doi: 10.1109/JQE.1966.1074006.
- [69] D. Pohl and W. Kaiser. Time-resolved investigations of stimulated brillouin scattering in transparent and absorbing media: Determination of phonon lifetimes. *Phys. Rev. B*, 1: 31–43, Jan 1970. doi:10.1103/PhysRevB.1.31. URL <https://link.aps.org/doi/10.1103/PhysRevB.1.31>.
- [70] Carlo E. Bottani and Daniele Fioretto. Brillouin scattering of phonons in complex materials. *Advances in Physics: X*, 3(1):1467281, 2018. doi:10.1080/23746149.2018.1467281. URL <https://doi.org/10.1080/23746149.2018.1467281>.
- [71] Andrew Briggs. *Advances in acoustic microscopy*, volume 1. Springer Science & Business Media, 2013.
- [72] D. Heiman, D. S. Hamilton, and R. W. Hellwarth. Brillouin scattering measurements on optical glasses. *Phys. Rev. B*, 19:6583–6592, Jun 1979. doi:10.1103/PhysRevB.19.6583. URL <https://link.aps.org/doi/10.1103/PhysRevB.19.6583>.
- [73] A. Link, R. Sooryakumar, R. S. Bandhu, and G. A. Antonelli. Brillouin light scattering studies of the mechanical properties of ultrathin low-k dielectric films. *Journal of Applied Physics*, 100(1):013507, 07 2006. ISSN 0021-8979. doi:10.1063/1.2209428. URL <https://doi.org/10.1063/1.2209428>.
- [74] Simin Pang, Xinbao Liu, Jiajun Luo, Yaru Xie, Jiang Tang, Sheng Meng, Ping-Heng Tan, and Jun Zhang. Brillouin light scattering of halide double perovskite. *Advanced Photonics Research*, 3(8):2100222, 2022. doi:<https://doi.org/10.1002/adpr.202100222>. URL <https://advanced.onlinelibrary.wiley.com/doi/abs/10.1002/adpr.202100222>.
- [75] P. Mutti, C. E. Bottani, G. Ghislotti, M. Beghi, G. A. D. Briggs, and J. R. Sandercock. *Surface Brillouin Scattering—Extending Surface Wave Measurements to 20 GHz*, pages 249–300. Springer US, Boston, MA, 1995. ISBN 978-1-4615-1873-0. doi:10.1007/978-1-4615-1873-

- 0_7. URL https://doi.org/10.1007/978-1-4615-1873-0_7.
- [76] J. R. Sandercock. *Trends in brillouin scattering: Studies of opaque materials, supported films, and central modes*, pages 173–206. Springer Berlin Heidelberg, Berlin, Heidelberg, 1982. ISBN 978-3-540-39208-8. doi:10.1007/3540115137_6. URL https://doi.org/10.1007/3540115137_6.
- [77] Daniel R. Birt, Kyongmo An, Annie Weathers, Li Shi, Maxim Tsoi, and Xiaoqin Li. Brillouin light scattering spectra as local temperature sensors for thermal magnons and acoustic phonons. *Applied Physics Letters*, 102(8):082401, 02 2013. ISSN 0003-6951. doi: 10.1063/1.4793538. URL <https://doi.org/10.1063/1.4793538>.
- [78] B. Hillebrands, P. Baumgart, and G. Güntherodt. In situ brillouin scattering from surface-anisotropy-dominated damon-eshbach modes in ultrathin epitaxial fe(110) layers. *Phys. Rev. B*, 36:2450–2453, Aug 1987. doi:10.1103/PhysRevB.36.2450. URL <https://link.aps.org/doi/10.1103/PhysRevB.36.2450>.
- [79] Burkard Hillebrands. Progress in multipass tandem fabry–perot interferometry: I. a fully automated, easy to use, self-aligning spectrometer with increased stability and flexibility. *Review of Scientific Instruments*, 70(3):1589–1598, 03 1999. ISSN 0034-6748. doi:10.1063/1.1149637. URL <https://doi.org/10.1063/1.1149637>.
- [80] Moritz Geilen, Felix Kohl, Alexandra Nicoloiu, Alexandru Müller, Burkard Hillebrands, and Philipp Pirro. Interference of co-propagating rayleigh and sezawa waves observed with micro-focused brillouin light scattering spectroscopy. *Applied Physics Letters*, 117(21):213501, 11 2020. ISSN 0003-6951. doi:10.1063/5.0029308. URL <https://doi.org/10.1063/5.0029308>.
- [81] Jie Yang, Meng-Ying Guo, Zong-Lin Li, Peng Wu, Kai-Ming Cai, Xiao-Ze Liu, Yu-Gui Peng, Qi Wang, and Xue-Feng Zhu. Brillouin-light-scattering imaging of undistorted field distribution and space-time evolution for gigahertz surface phonons. *Phys. Rev. Appl.*, 23:L051001, May 2025. doi:10.1103/PhysRevApplied.23.L051001. URL <https://link.aps.org/doi/10.1103/PhysRevApplied.23.L051001>.
- [82] Marco Madami, Gianluca Gubbiotti, Silvia Tacchi, and Giovanni Carlotti. Chapter two - application of microfocused brillouin light scattering to the study of spin waves in low-dimensional magnetic systems. volume 63 of *Solid State Physics*, pages 79–150. Academic Press, 2012. doi:<https://doi.org/10.1016/B978-0-12-397028-2.00002-3>. URL <https://www.sciencedirect.com/science/article/pii/B9780123970282000023>.

- [83] Michael Guerette and Liping Huang. A simple and convenient set-up for high-temperature brillouin light scattering. *Journal of Physics D: Applied Physics*, 45(27):275302, jun 2012. doi:10.1088/0022-3727/45/27/275302. URL <https://dx.doi.org/10.1088/0022-3727/45/27/275302>.
- [84] Irina V Kabakova, Ido Azuri, Zhuoying Chen, Pabitra K Nayak, Henry J Snaith, Leeor Kronik, Carl Paterson, Artem A Bakulin, and David A Egger. The effect of ionic composition on acoustic phonon speeds in hybrid perovskites from brillouin spectroscopy and density functional theory. *Journal of Materials Chemistry C*, 6(15):3861–3868, 2018. doi: 10.1039/C8TC00875B. URL <http://dx.doi.org/10.1039/C8TC00875B>.
- [85] M. H. Grimsditch and A. K. Ramdas. Brillouin scattering in diamond. *Phys. Rev. B*, 11: 3139–3148, Apr 1975. doi:10.1103/PhysRevB.11.3139. URL <https://link.aps.org/doi/10.1103/PhysRevB.11.3139>.
- [86] R. Vacher and L. Boyer. Brillouin scattering: A tool for the measurement of elastic and photoelastic constants. *Phys. Rev. B*, 6:639–673, Jul 1972. doi:10.1103/PhysRevB.6.639. URL <https://link.aps.org/doi/10.1103/PhysRevB.6.639>.
- [87] Charles H. Whitfield, Edward M. Brody, and William A. Bassett. Elastic moduli of nacl by brillouin scattering at high pressure in a diamond anvil cell. *Review of Scientific Instruments*, 47(8):942–947, 08 1976. ISSN 0034-6748. doi:10.1063/1.1134778. URL <https://doi.org/10.1063/1.1134778>.
- [88] M. Yamaguchi, T. Yagi, T. Sota, T. Deguchi, K. Shimada, and S. Nakamura. Brillouin scattering study of bulk gan. *Journal of Applied Physics*, 85(12):8502–8504, 06 1999. ISSN 0021-8979. doi:10.1063/1.370635. URL <https://doi.org/10.1063/1.370635>.
- [89] Chang-Sheng Zha, Ho kwang Mao, and Russell J. Hemley. Elasticity of mgo and a primary pressure scale to 55 gpa. *Proceedings of the National Academy of Sciences*, 97(25):13494–13499, 2000. doi:10.1073/pnas.240466697. URL <https://www.pnas.org/doi/abs/10.1073/pnas.240466697>.
- [90] Fuming Jiang, Gabriel D. Gwanmesia, Tatiyana I. Dyuzheva, and Thomas S. Duffy. Elasticity of stishovite and acoustic mode softening under high pressure by brillouin scattering. *Physics of the Earth and Planetary Interiors*, 172(3):235–240, 2009. ISSN 0031-9201. doi:<https://doi.org/10.1016/j.pepi.2008.09.017>. URL <https://www.sciencedirect.com/science/article/pii/S003192010800277X>.

- [91] Samuel Raetz, Maju Kuriakose, Philippe Djemia, Sergey M. Nikitin, Nikolay Chigarev, Vincent Tournat, Alain Bulou, Alexey Lomonosov, Vitalyi E. Gusev, and Andreas Zerr. Elastic anisotropy and single-crystal moduli of solid argon up to 64 gpa from time-domain brillouin scattering. *Phys. Rev. B*, 99:224102, Jun 2019. doi:10.1103/PhysRevB.99.224102. URL <https://link.aps.org/doi/10.1103/PhysRevB.99.224102>.
- [92] A. Kurnosov, G. Criniti, T. Boffa Ballaran, H. Marquardt, and D. J. Frost. High pressure and high temperature brillouin scattering measurements of pyrope single crystals using flexible co₂ laser heating systems. *Physics and Chemistry of Minerals*, 51(4):38, Oct 2024. ISSN 1432-2021. doi:10.1007/s00269-024-01297-2. URL <https://doi.org/10.1007/s00269-024-01297-2>.
- [93] V. V. Brazhkin and A. G. Lyapin. Elastic properties of substances in the megabar pressure range: Inversion of shear rigidity. *Journal of Experimental and Theoretical Physics Letters*, 73(4):197–201, Feb 2001. ISSN 1090-6487. doi:10.1134/1.1368714. URL <https://doi.org/10.1134/1.1368714>.
- [94] M. Grimsditch, P. Loubeyre, and A. Polian. Brillouin scattering and three-body forces in argon at high pressures. *Phys. Rev. B*, 33:7192–7200, May 1986. doi:10.1103/PhysRevB.33.7192. URL <https://link.aps.org/doi/10.1103/PhysRevB.33.7192>.
- [95] A. Polian, J. M. Besson, M. Grimsditch, and H. Vogt. Elastic properties of gas under high pressure by brillouin scattering. *Phys. Rev. B*, 25:2767–2775, Feb 1982. doi:10.1103/PhysRevB.25.2767. URL <https://link.aps.org/doi/10.1103/PhysRevB.25.2767>.
- [96] E. S. Zouboulis, M. Grimsditch, A. K. Ramdas, and S. Rodriguez. Temperature dependence of the elastic moduli of diamond: A brillouin-scattering study. *Phys. Rev. B*, 57: 2889–2896, Feb 1998. doi:10.1103/PhysRevB.57.2889. URL <https://link.aps.org/doi/10.1103/PhysRevB.57.2889>.
- [97] Lewis L. Stevens and Craig J. Eckhardt. The elastic constants and related properties of β-hmx determined by brillouin scattering. *The Journal of Chemical Physics*, 122(17):174701, 04 2005. ISSN 0021-9606. doi:10.1063/1.1883627. URL <https://doi.org/10.1063/1.1883627>.
- [98] Jin-Chong Tan, Bartolomeo Civalleri, Chung-Cherng Lin, Loredana Valenzano, Raimondas Galvelis, Po-Fei Chen, Thomas D. Bennett, Caroline Mellot-Draznieks, Claudio M. Zicovich-Wilson, and Anthony K. Cheetham. Exceptionally low shear modulus in a pro-

- totypical imidazole-based metal-organic framework. *Phys. Rev. Lett.*, 108:095502, Feb 2012. doi:10.1103/PhysRevLett.108.095502. URL <https://link.aps.org/doi/10.1103/PhysRevLett.108.095502>.
- [99] Carmen Sanchez-Valle, Stanislav V. Sinogeikin, Zoe A. D. Lethbridge, Richard I. Walton, Christopher W. Smith, Kenneth E. Evans, and Jay D. Bass. Brillouin scattering study on the single-crystal elastic properties of natrolite and analcime zeolites. *Journal of Applied Physics*, 98(5):053508, 09 2005. ISSN 0021-8979. doi:10.1063/1.2014932. URL <https://doi.org/10.1063/1.2014932>.
- [100] G. Dirras, L. Lilensten, P. Djemia, M. Laurent-Brocq, D. Tingaud, J.-P. Couzinié, L. Perrière, T. Chauveau, and I. Guillot. Elastic and plastic properties of as-cast equimolar tihfzrtanb high-entropy alloy. *Materials Science and Engineering: A*, 654:30–38, 2016. ISSN 0921-5093. doi:<https://doi.org/10.1016/j.msea.2015.12.017>. URL <https://www.sciencedirect.com/science/article/pii/S0921509315307140>.
- [101] J. Baranowski, B. Mroz, S. Mielcarek, I. Iatsunskyi, and A. Trzaskowska. High resolution brillouin spectroscopy of the surface acoustic waves in sb₂te₃ van der waals single crystals. *Scientific Reports*, 15(1):1358, Jan 2025. ISSN 2045-2322. doi:10.1038/s41598-025-85742-4. URL <https://doi.org/10.1038/s41598-025-85742-4>.
- [102] D. Faurie, P. Djemia, E. Le Bourhis, P.-O. Renault, Y. Roussigné, S.M. Chérif, R. Brenner, O. Castelnau, G. Patriarche, and Ph. Goudeau. Elastic anisotropy of polycrystalline au films: Modeling and respective contributions of x-ray diffraction, nanoindentation and brillouin light scattering. *Acta Materialia*, 58(15):4998–5008, 2010. ISSN 1359-6454. doi:<https://doi.org/10.1016/j.actamat.2010.05.034>. URL <https://www.sciencedirect.com/science/article/pii/S1359645410003198>.
- [103] R. J. Jimenez-Rioboo, L. Artus, R. Cusco, T. Taniguchi, G. Cassabois, and B. Gil. In- and out-of-plane longitudinal acoustic-wave velocities and elastic moduli in h-bn from brillouin scattering measurements. *Applied Physics Letters*, 112(5):051905, 01 2018. ISSN 0003-6951. doi:10.1063/1.5019629. URL <https://doi.org/10.1063/1.5019629>.
- [104] Bryan W. Reed and Kristie J. Koski. Acoustic phonons and elastic stiffnesses from brillouin scattering of cdps₃. *Journal of Applied Physics*, 131(16):165109, 04 2022. ISSN 0021-8979. doi:10.1063/5.0084258. URL <https://doi.org/10.1063/5.0084258>.

- [105] Bryan W. Reed, Ethan Chen, and Kristie J. Koski. Tunable chemochromism and elastic properties in intercalated moo_3 : Au-, cr-, fe-, ge-, mn-, and ni- moo_3 . *ACS Nano*, 18(20):12845–12852, May 2024. ISSN 1936-0851. doi:10.1021/acsnano.4c00016. URL <https://doi.org/10.1021/acsnano.4c00016>.
- [106] Visnja Babacic, David Saleta Reig, Sebin Varghese, Thomas Vasileiadis, Emerson Coy, Klaas-Jan Tielrooij, and Bartlomiej Graczykowski. Thickness-dependent elastic softening of few-layer free-standing mose_2 . *Advanced Materials*, 33(23):2008614, 2021. doi: <https://doi.org/10.1002/adma.202008614>. URL <https://advanced.onlinelibrary.wiley.com/doi/abs/10.1002/adma.202008614>.
- [107] Brent Perreault, Johannes Knolle, Natalia B. Perkins, and F. J. Burnell. Resonant raman scattering theory for kitaev models and their majorana fermion boundary modes. *Phys. Rev. B*, 94:104427, Sep 2016. doi:10.1103/PhysRevB.94.104427. URL <https://link.aps.org/doi/10.1103/PhysRevB.94.104427>.
- [108] Alexander A. Balandin and Denis L. Nika. Phononics in low-dimensional materials. *Materials Today*, 15(6):266–275, 2012. ISSN 1369-7021. doi:[https://doi.org/10.1016/S1369-7021\(12\)70117-7](https://doi.org/10.1016/S1369-7021(12)70117-7). URL <https://www.sciencedirect.com/science/article/pii/S1369702112701177>.
- [109] V. L. Zhang, C. G. Hou, H. H. Pan, F. S. Ma, M. H. Kuok, H. S. Lim, S. C. Ng, M. G. Cottam, M. Jamali, and H. Yang. Phononic dispersion of a two-dimensional chessboard-patterned bicomponent array on a substrate. *Applied Physics Letters*, 101(5):053102, 07 2012. ISSN 0003-6951. doi:10.1063/1.4739950. URL <https://doi.org/10.1063/1.4739950>.
- [110] C. G. Hou, V. L. Zhang, S. C. Ng, M. H. Kuok, H. S. Lim, X. M. Liu, and A. O. Adeyeye. Dispersion and origin of surface optical-like waves in a two-dimensional antidot-patterned structure with a soft intervening layer. *Applied Physics Letters*, 104(9):093108, 03 2014. ISSN 0003-6951. doi:10.1063/1.4868020. URL <https://doi.org/10.1063/1.4868020>.
- [111] Slawomir Mielcarek, Aleksandra Trzaskowska, Bartlomiej Graczykowski, and Jayanta Sarkar. Hypersonic surface waves in 2d titanium nanostructure on silicon. *physica status solidi (RRL) – Rapid Research Letters*, 6(4):175–177, 2012. doi:<https://doi.org/10.1002/pssr.201206039>. URL <https://onlinelibrary.wiley.com/doi/abs/10.1002/pssr.201206039>.
- [112] B. Graczykowski, S. Mielcarek, A. Trzaskowska, J. Sarkar, P. Hakonen, and B. Mroz. Tuning of a hypersonic surface phononic band gap using a nanoscale two-dimensional lattice of pillars.

Phys. Rev. B, 86:085426, Aug 2012. doi:10.1103/PhysRevB.86.085426. URL <https://link.aps.org/doi/10.1103/PhysRevB.86.085426>.

- [113] Zahra Ebrahim Nataj, Youming Xu, Dylan Wright, Jonas O. Brown, Jivtesh Garg, Xi Chen, Fariborz Kargar, and Alexander A. Balandin. Cryogenic characteristics of graphene composites—evolution from thermal conductors to thermal insulators. *Nature Communications*, 14(1):3190, Jun 2023. ISSN 2041-1723. doi:10.1038/s41467-023-38508-3. URL <https://doi.org/10.1038/s41467-023-38508-3>.
- [114] Chun Yu Tammy Huang, Fariborz Kargar, Topojit Debnath, Bishwajit Debnath, Michael D Valentin, Ron Synowicki, Stefan Schoeche, Roger K Lake, and Alexander A Balandin. Phononic and photonic properties of shape-engineered silicon nanoscale pillar arrays. *Nanotechnology*, 31(30):30LT01, may 2020. doi:10.1088/1361-6528/ab85ee. URL <https://dx.doi.org/10.1088/1361-6528/ab85ee>.
- [115] Dylan Wright, Zahra Ebrahim Nataj, Erick Guzman, Jake Polster, Menno Bouman, Fariborz Kargar, and Alexander A. Balandin. Acoustic and optical phonons in quasi-two-dimensional mps3 antiferromagnetic semiconductors. *Applied Physics Letters*, 124(16):161903, 04 2024. ISSN 0003-6951. doi:10.1063/5.0205946. URL <https://doi.org/10.1063/5.0205946>.
- [116] D. Yudistira, A. Boes, B. Graczykowski, F. Alzina, L. Y. Yeo, C. M. Sotomayor Torres, and A. Mitchell. Nanoscale pillar hypersonic surface phononic crystals. *Phys. Rev. B*, 94:094304, Sep 2016. doi:10.1103/PhysRevB.94.094304. URL <https://link.aps.org/doi/10.1103/PhysRevB.94.094304>.
- [117] B. Graczykowski, M. Sledzinska, F. Alzina, J. Gomis-Bresco, J. S. Reparaz, M. R. Wagner, and C. M. Sotomayor Torres. Phonon dispersion in hypersonic two-dimensional phononic crystal membranes. *Phys. Rev. B*, 91:075414, Feb 2015. doi:10.1103/PhysRevB.91.075414. URL <https://link.aps.org/doi/10.1103/PhysRevB.91.075414>.
- [118] Marianna Sledzinska, Bartłomiej Graczykowski, Jeremie Maire, Emigdio Chavez-Angel, Clivia M. Sotomayor-Torres, and Francesc Alzina. 2d phononic crystals: Progress and prospects in hypersound and thermal transport engineering. *Advanced Functional Materials*, 30(8):1904434, 2020. doi:<https://doi.org/10.1002/adfm.201904434>. URL <https://advanced.onlinelibrary.wiley.com/doi/abs/10.1002/adfm.201904434>.
- [119] Alexander Balandin and Kang L. Wang. Significant decrease of the lattice thermal conductivity due to phonon confinement in a free-standing semiconductor quantum well. *Phys. Rev.*

- B*, 58:1544–1549, Jul 1998. doi:10.1103/PhysRevB.58.1544. URL <https://link.aps.org/doi/10.1103/PhysRevB.58.1544>.
- [120] Fariborz Kargar, Sylvester Ramirez, Bishwajit Debnath, Hoda Malekpour, Roger K. Lake, and Alexander A. Balandin. Acoustic phonon spectrum and thermal transport in nanoporous alumina arrays. *Applied Physics Letters*, 107(17):171904, 10 2015. ISSN 0003-6951. doi: 10.1063/1.4934883. URL <https://doi.org/10.1063/1.4934883>.
- [121] John Cuffe, Emigdio Chávez, Andrey Shchepetov, Pierre-Olivier Chapuis, El Houssaine El Boudouti, Francesc Alzina, Timothy Kehoe, Jordi Gomis-Bresco, Damian Dudek, Yan Pennec, Bahram Djafari-Rouhani, Mika Prunnila, Jouni Ahopelto, and Clivia M. Sotomayor Torres. Phonons in slow motion: Dispersion relations in ultrathin si membranes. *Nano Letters*, 12(7):3569–3573, Jul 2012. ISSN 1530-6984. doi:10.1021/nl301204u. URL <https://doi.org/10.1021/nl301204u>.
- [122] Sanghamitra Neogi, J. Sebastian Reparaz, Luiz Felipe C. Pereira, Bartłomiej Graczykowski, Markus R. Wagner, Marianna Sledzinska, Andrey Shchepetov, Mika Prunnila, Jouni Ahopelto, Clivia M. Sotomayor-Torres, and Davide Donadio. Tuning thermal transport in ultrathin silicon membranes by surface nanoscale engineering. *ACS Nano*, 9(4):3820–3828, Apr 2015. ISSN 1936-0851. doi:10.1021/nn506792d. URL <https://doi.org/10.1021/nn506792d>.
- [123] Bryan W. Reed, Daniel R. Williams, Bryan P. Moser, and Kristie J. Koski. Chemically tuning quantized acoustic phonons in 2d layered moo_3 nanoribbons. *Nano Letters*, 19(7):4406–4412, Jul 2019. ISSN 1530-6984. doi:10.1021/acs.nanolett.9b01068. URL <https://doi.org/10.1021/acs.nanolett.9b01068>.
- [124] J. Sandercock and W. Wetling. Light scattering from thermal magnons in iron and nickel. *IEEE Transactions on Magnetics*, 14(5):442–444, 1978. doi:10.1109/TMAG.1978.1059895.
- [125] M. Grimsditch, A. Malozemoff, and A. Brunsch. Standing spin waves observed by brillouin scattering in amorphous metallic $\text{fe}_{80}\text{b}_{20}$ films. *Phys. Rev. Lett.*, 43:711–714, Sep 1979. doi: 10.1103/PhysRevLett.43.711. URL <https://link.aps.org/doi/10.1103/PhysRevLett.43.711>.
- [126] Kyongmo An, Daniel R. Birt, Chi-Feng Pai, Kevin Olsson, Daniel C. Ralph, Robert A. Buhrman, and Xiaoqin Li. Control of propagating spin waves via spin transfer torque in a metallic bilayer waveguide. *Phys. Rev. B*, 89:140405, Apr 2014. doi: 10.1103/PhysRevB.89.140405. URL <https://link.aps.org/doi/10.1103/PhysRevB.89.140405>.

140405.

- [127] A. A. Stashkevich, M. Belmeguenai, Y. Roussigné, S. M. Cherif, M. Kostylev, M. Gabor, D. Lacour, C. Tiusan, and M. Hehn. Experimental study of spin-wave dispersion in py/pt film structures in the presence of an interface dzyaloshinskii-moriya interaction. *Phys. Rev. B*, 91:214409, Jun 2015. doi:10.1103/PhysRevB.91.214409. URL <https://link.aps.org/doi/10.1103/PhysRevB.91.214409>.
- [128] Xin Ma, Guoqiang Yu, Chi Tang, Xiang Li, Congli He, Jing Shi, Kang L. Wang, and Xiaoqin Li. Interfacial dzyaloshinskii-moriya interaction: Effect of 5d band filling and correlation with spin mixing conductance. *Phys. Rev. Lett.*, 120:157204, Apr 2018. doi:10.1103/PhysRevLett.120.157204. URL <https://link.aps.org/doi/10.1103/PhysRevLett.120.157204>.
- [129] K. Vogt, H. Schultheiss, S. J. Hermsdoerfer, P. Pirro, A. A. Serga, and B. Hillebrands. All-optical detection of phase fronts of propagating spin waves in a ni₈fe₁9 microstripe. *Applied Physics Letters*, 95(18):182508, 11 2009. ISSN 0003-6951. doi:10.1063/1.3262348. URL <https://doi.org/10.1063/1.3262348>.
- [130] Vladislav E. Demidov and Sergej O. Demokritov. Magnonic waveguides studied by micro-focus brillouin light scattering. *IEEE Transactions on Magnetics*, 51(4):1–15, 2015. doi:10.1109/TMAG.2014.2388196.
- [131] M. Agrawal, V. I. Vasyuchka, A. A. Serga, A. D. Karenowska, G. A. Melkov, and B. Hillebrands. Direct measurement of magnon temperature: New insight into magnon-phonon coupling in magnetic insulators. *Phys. Rev. Lett.*, 111:107204, Sep 2013. doi:10.1103/PhysRevLett.111.107204. URL <https://link.aps.org/doi/10.1103/PhysRevLett.111.107204>.
- [132] Chenbo Zhao, Zhizhi Zhang, Yi Li, Wei Zhang, John E. Pearson, Ralu Diwan, Qingfang Liu, Valentine Novosad, Jianbo Wang, and Axel Hoffmann. Direct imaging of resonant phonon-magnon coupling. *Phys. Rev. Appl.*, 15:014052, Jan 2021. doi:10.1103/PhysRevApplied.15.014052. URL <https://link.aps.org/doi/10.1103/PhysRevApplied.15.014052>.
- [133] José Holanda, Daniel S. Maior, Obed Alves Santos, Antonio Azevedo, and Sergio M. Rezende. Evidence of phonon pumping by magnonic spin currents. *Applied Physics Letters*, 118(2):022409, 01 2021. ISSN 0003-6951. doi:10.1063/5.0035690. URL <https://doi.org/10.1063/5.0035690>.

5.0035690.

- [134] Yannik Kunz, Matthias Küß, Michael Schneider, Moritz Geilen, Philipp Pirro, Manfred Albrecht, and Mathias Weiler. Coherent surface acoustic wave–spin wave interactions detected by micro-focused brillouin light scattering spectroscopy. *Applied Physics Letters*, 124(15):152403, 04 2024. ISSN 0003-6951. doi:10.1063/5.0189324. URL <https://doi.org/10.1063/5.0189324>.
- [135] S.O. Demokritov, B. Hillebrands, and A.N. Slavin. Brillouin light scattering studies of confined spin waves: linear and nonlinear confinement. *Physics Reports*, 348(6):441–489, 2001. ISSN 0370-1573. doi:[https://doi.org/10.1016/S0370-1573\(00\)00116-2](https://doi.org/10.1016/S0370-1573(00)00116-2). URL <https://www.sciencedirect.com/science/article/pii/S0370157300001162>.
- [136] Hanchen Wang, Marco Madami, Jilei Chen, Hao Jia, Yu Zhang, Rundong Yuan, Yizhan Wang, Wenqing He, Lutong Sheng, Yuelin Zhang, Jinlong Wang, Song Liu, Ka Shen, Guoqiang Yu, Xiufeng Han, Dapeng Yu, Jean-Philippe Ansermet, Gianluca Gubbiotti, and Haiming Yu. Observation of spin-wave moiré edge and cavity modes in twisted magnetic lattices. *Phys. Rev. X*, 13:021016, Apr 2023. doi:10.1103/PhysRevX.13.021016. URL <https://link.aps.org/doi/10.1103/PhysRevX.13.021016>.
- [137] Vladislav E. Demidov, Sergej O. Demokritov, Karsten Rott, Patryk Krzysteczko, and Guenter Reiss. Nano-optics with spin waves at microwave frequencies. *Applied Physics Letters*, 92(23):232503, 06 2008. ISSN 0003-6951. doi:10.1063/1.2945000. URL <https://doi.org/10.1063/1.2945000>.
- [138] Fariborz Kargar, Michael Balinskiy, Howard Chiang, Andres C. Chavez, John Nance, Alexander Khitun, Gregory P. Carman, and Alexander A. Balandin. Brillouin-mandelstam spectroscopy of stress-modulated spatially confined spin waves in ni thin films on piezoelectric substrates. *Journal of Magnetism and Magnetic Materials*, 501:166440, 2020. ISSN 0304-8853. doi:<https://doi.org/10.1016/j.jmmm.2020.166440>. URL <https://www.sciencedirect.com/science/article/pii/S0304885319339782>.
- [139] Hans Joachim Eichler, Peter Günter, and Dieter W Pohl. *Laser-induced dynamic gratings*, volume 50. Springer, 2013.
- [140] Norman M. Kroll. Excitation of hypersonic vibrations by means of photoelastic coupling of high-intensity light waves to elastic waves. *Journal of Applied Physics*, 36(1):34–43, 01 1965. ISSN 0021-8979. doi:10.1063/1.1713918. URL <https://doi.org/10.1063/1.1713918>.

- [141] Jean-Charles Beugnot and Vincent Laude. Electrostriction and guidance of acoustic phonons in optical fibers. *Phys. Rev. B*, 86:224304, Dec 2012. doi:10.1103/PhysRevB.86.224304. URL <https://link.aps.org/doi/10.1103/PhysRevB.86.224304>.
- [142] R. M. Herman and M. A. Gray. Theoretical prediction of the stimulated thermal rayleigh scattering in liquids. *Phys. Rev. Lett.*, 19:824–828, Oct 1967. doi:10.1103/PhysRevLett.19.824. URL <https://link.aps.org/doi/10.1103/PhysRevLett.19.824>.
- [143] Darius H. Torchinsky, Jeremy A. Johnson, and Keith A. Nelson. A direct test of the correlation between elastic parameters and fragility of ten glass formers and their relationship to elastic models of the glass transition. *The Journal of Chemical Physics*, 130(6):064502, 02 2009. ISSN 0021-9606. doi:10.1063/1.3072476. URL <https://doi.org/10.1063/1.3072476>.
- [144] John A. Rogers, Alex Maznev, and Keith A. Nelson. *Impulsive Stimulated Thermal Scattering*, pages 1–17. John Wiley & Sons, Ltd, 2012. ISBN 9780471266969. doi: <https://doi.org/10.1002/0471266965.com063.pub2>. URL <https://onlinelibrary.wiley.com/doi/abs/10.1002/0471266965.com063.pub2>.
- [145] Usama Choudhry, Taeyong Kim, Melanie Adams, Jeewan Ranasinghe, Runqing Yang, and Bolin Liao. Characterizing microscale energy transport in materials with transient grating spectroscopy. *Journal of Applied Physics*, 130(23):231101, 12 2021. ISSN 0021-8979. doi: 10.1063/5.0068915. URL <https://doi.org/10.1063/5.0068915>.
- [146] Taeyong Kim, Ding Ding, Jong-Hyuk Yim, Young-Dahl Jho, and Austin J. Minnich. Elastic and thermal properties of free-standing molybdenum disulfide membranes measured using ultrafast transient grating spectroscopy. *APL Materials*, 5(8):086105, 08 2017. ISSN 2166-532X. doi:10.1063/1.4999225. URL <https://doi.org/10.1063/1.4999225>.
- [147] A. A. Maznev, K. A. Nelson, and J. A. Rogers. Optical heterodyne detection of laser-induced gratings. *Opt. Lett.*, 23(16):1319–1321, Aug 1998. doi:10.1364/OL.23.001319. URL <https://opg.optica.org/ol/abstract.cfm?URI=ol-23-16-1319>.
- [148] A. A. Maznev and A. G. Every. Surface acoustic waves with negative group velocity in a thin film structure on silicon. *Applied Physics Letters*, 95(1):011903, 07 2009. ISSN 0003-6951. doi:10.1063/1.3168509. URL <https://doi.org/10.1063/1.3168509>.
- [149] A. A. Maznev and O. B. Wright. Optical generation of long-lived surface vibrations in a periodic microstructure. *Journal of Applied Physics*, 105(12):123530, 06 2009. ISSN 0021-8979. doi:10.1063/1.3153956. URL <https://doi.org/10.1063/1.3153956>.

- [150] N. Boechler, J. K. Eliason, A. Kumar, A. A. Maznev, K. A. Nelson, and N. Fang. Interaction of a contact resonance of microspheres with surface acoustic waves. *Phys. Rev. Lett.*, 111:036103, Jul 2013. doi:10.1103/PhysRevLett.111.036103. URL <https://link.aps.org/doi/10.1103/PhysRevLett.111.036103>.
- [151] A. A. Maznev and A. G. Every. Surface acoustic waves in a periodically patterned layered structure. *Journal of Applied Physics*, 106(11):113531, 12 2009. ISSN 0021-8979. doi: 10.1063/1.3267290. URL <https://doi.org/10.1063/1.3267290>.
- [152] M. J. Simmonds, A. Založnik, M. I. Patino, M. J. Baldwin, and N. Boechler. An increased accuracy laser-induced transient grating spectroscopy analysis method for probing near surface thermal diffusivity with gigahertz frequency instrumentation. *AIP Advances*, 14(10):105226, 10 2024. ISSN 2158-3226. doi:10.1063/5.0196820. URL <https://doi.org/10.1063/5.0196820>.
- [153] Yongwu Yang and Keith A. Nelson. Impulsive stimulated light scattered from glass-forming liquids. ii. salol relaxation dynamics, nonergodicity parameter, and testing of mode coupling theory. *The Journal of Chemical Physics*, 103(18):7732–7739, 11 1995. ISSN 0021-9606. doi:10.1063/1.470294. URL <https://doi.org/10.1063/1.470294>.
- [154] Yong-Xin Yan, Lap-Tak Cheng, and Keith A. Nelson. The temperature-dependent distribution of relaxation times in glycerol: Time-domain light scattering study of acoustic and mountain-mode behavior in the 20 mhz-3 ghz frequency range. *The Journal of Chemical Physics*, 88(10):6477–6486, 05 1988. ISSN 0021-9606. doi:10.1063/1.454433. URL <https://doi.org/10.1063/1.454433>.
- [155] Dora M. Paolucci and Keith A. Nelson. Impulsive stimulated thermal scattering study of structural relaxation in supercooled glycerol. *The Journal of Chemical Physics*, 112(15):6725–6732, 04 2000. ISSN 0021-9606. doi:10.1063/1.481248. URL <https://doi.org/10.1063/1.481248>.
- [156] A. Steigerwald, Y. Xu, J. Qi, J. Gregory, X. Liu, J. K. Furdyna, K. Varga, A. B. Hmelo, G. Lüpke, L. C. Feldman, and N. Tolk. Semiconductor point defect concentration profiles measured using coherent acoustic phonon waves. *Applied Physics Letters*, 94(11):111910, 03 2009. ISSN 0003-6951. doi:10.1063/1.3099341. URL <https://doi.org/10.1063/1.3099341>.
- [157] C. Mechri, P. Ruello, J. M. Breteau, M. R. Baklanov, P. Verdonck, and V. Gusev. Depth-profiling of elastic inhomogeneities in transparent nanoporous low-k materials by picosecond

- ultrasonic interferometry. *Applied Physics Letters*, 95(9):091907, 09 2009. ISSN 0003-6951. doi:10.1063/1.3220063. URL <https://doi.org/10.1063/1.3220063>.
- [158] J. J. Kasinski, L. A. Gomez-Jahn, K. J. Faran, S. M. Gracewski, and R. J. Dwayne Miller. Picosecond dynamics of surface electron transfer processes: Surface restricted transient grating studies of the *n*-tio₂/h₂o interface. *The Journal of Chemical Physics*, 90(2):1253–1269, 01 1989. ISSN 0021-9606. doi:10.1063/1.456130. URL <https://doi.org/10.1063/1.456130>.
- [159] C. Glorieux, K. Van de Rostyne, J. Goossens, G. Shkerdin, W. Lauriks, and K. A. Nelson. Shear properties of glycerol by interface wave laser ultrasonics. *Journal of Applied Physics*, 99(1):013511, 01 2006. ISSN 0021-8979. doi:10.1063/1.2150257. URL <https://doi.org/10.1063/1.2150257>.
- [160] J. Sermeus, R. Sinha, K. Vanstreels, P. M. Vereecken, and C. Glorieux. Determination of elastic properties of a mno₂ coating by surface acoustic wave velocity dispersion analysis. *Journal of Applied Physics*, 116(2):023503, 07 2014. ISSN 0021-8979. doi:10.1063/1.4885427. URL <https://doi.org/10.1063/1.4885427>.
- [161] I. Malfanti, A. Taschin, P. Bartolini, B. Bonello, and R. Torre. Propagation of acoustic surface waves on a phononic surface investigated by transient reflecting grating spectroscopy. *Journal of the Mechanics and Physics of Solids*, 59(11):2370–2381, 2011. ISSN 0022-5096. doi:<https://doi.org/10.1016/j.jmps.2011.07.010>. URL <https://www.sciencedirect.com/science/article/pii/S0022509611001645>.
- [162] J. K. Eliason, A. Vega-Flick, M. Hiraiwa, A. Khanolkar, T. Gan, N. Boechler, N. Fang, K. A. Nelson, and A. A. Maznev. Resonant attenuation of surface acoustic waves by a disordered monolayer of microspheres. *Applied Physics Letters*, 108(6):061907, 02 2016. ISSN 0003-6951. doi:10.1063/1.4941808. URL <https://doi.org/10.1063/1.4941808>.
- [163] A. Vega-Flick, R. A. Duncan, S. P. Wallen, N. Boechler, C. Stelling, M. Retsch, J. J. Alvarado-Gil, K. A. Nelson, and A. A. Maznev. Vibrational dynamics of a two-dimensional microgranular crystal. *Phys. Rev. B*, 96:024303, Jul 2017. doi:10.1103/PhysRevB.96.024303. URL <https://link.aps.org/doi/10.1103/PhysRevB.96.024303>.
- [164] Benedikt Krug, Nektarios Koukourakis, Jochen Guck, and Jürgen Czarske. Nonlinear microscopy using impulsive stimulated brillouin scattering for high-speed elastography. *Opt. Express*, 30(4):4748–4758, Feb 2022. doi:10.1364/OE.449980. URL <https://opg.optica.org/oe/abstract.cfm?URI=oe-30-4-4748>.

- [165] Jiarui Li, Taoran Le, Hongyuan Zhang, Haoyun Wei, and Yan Li. High-speed impulsive stimulated brillouin microscopy. *Photon. Res.*, 12(4):730–739, Apr 2024. doi:10.1364/PRJ.509922. URL <https://opg.optica.org/prj/abstract.cfm?URI=prj-12-4-730>.
- [166] Jiarui Li, Hongyuan Zhang, Minjian Lu, Haoyun Wei, and Yan Li. Sensitive impulsive stimulated brillouin spectroscopy by an adaptive noise-suppression matrix pencil. *Opt. Express*, 30(16):29598–29610, Aug 2022. doi:10.1364/OE.465106. URL <https://opg.optica.org/oe/abstract.cfm?URI=oe-30-16-29598>.
- [167] G. Wang, B. L. Liu, A. Balocchi, P. Renucci, C. R. Zhu, T. Amand, C. Fontaine, and X. Marie. Gate control of the electron spin-diffusion length in semiconductor quantum wells. *Nature Communications*, 4(1):2372, Sep 2013. ISSN 2041-1723. doi:10.1038/ncomms3372. URL <https://doi.org/10.1038/ncomms3372>.
- [168] M. P. Walser, C. Reichl, W. Wegscheider, and G. Salis. Direct mapping of the formation of a persistent spin helix. *Nature Physics*, 8(10):757–762, Oct 2012. ISSN 1745-2481. doi:10.1038/nphys2383. URL <https://doi.org/10.1038/nphys2383>.
- [169] Luyi Yang, J. D. Koralek, J. Orenstein, D. R. Tibbetts, J. L. Reno, and M. P. Lilly. Doppler velocimetry of spin propagation in a two-dimensional electron gas. *Nature Physics*, 8(2):153–157, Feb 2012. ISSN 1745-2481. doi:10.1038/nphys2157. URL <https://doi.org/10.1038/nphys2157>.
- [170] S. G. Carter, Z. Chen, and S. T. Cundiff. Optical measurement and control of spin diffusion in *n*-doped gaas quantum wells. *Phys. Rev. Lett.*, 97:136602, Sep 2006. doi:10.1103/PhysRevLett.97.136602. URL <https://link.aps.org/doi/10.1103/PhysRevLett.97.136602>.
- [171] Luyi Yang, J. D. Koralek, J. Orenstein, D. R. Tibbetts, J. L. Reno, and M. P. Lilly. Coherent propagation of spin helices in a quantum-well confined electron gas. *Phys. Rev. Lett.*, 109:246603, Dec 2012. doi:10.1103/PhysRevLett.109.246603. URL <https://link.aps.org/doi/10.1103/PhysRevLett.109.246603>.
- [172] T. Ishiguro, Y. Toda, and S. Adachi. Exciton spin relaxation in gan observed by spin grating experiment. *Applied Physics Letters*, 90(1):011904, 01 2007. ISSN 0003-6951. doi:10.1063/1.2430402. URL <https://doi.org/10.1063/1.2430402>.
- [173] T. Watanuki, S. Adachi, H. Sasakura, and S. Muto. Long spin relaxation in self-assembled inalas quantum dots observed by heterodyne four-wave mixing. *Applied Physics Letters*, 86

- (6):063114, 02 2005. ISSN 0003-6951. doi:10.1063/1.1861978. URL <https://doi.org/10.1063/1.1861978>.
- [174] Gregory D. Scholes, Jeongho Kim, and Cathy Y. Wong. Exciton spin relaxation in quantum dots measured using ultrafast transient polarization grating spectroscopy. *Phys. Rev. B*, 73:195325, May 2006. doi:10.1103/PhysRevB.73.195325. URL <https://link.aps.org/doi/10.1103/PhysRevB.73.195325>.
- [175] Jeongho Kim, Cathy Y. Wong, Sreekumari P. Nair, Karolina P. Fritz, Sandeep Kumar, and Gregory D. Scholes. Mechanism and origin of exciton spin relaxation in cdse nanorods. *The Journal of Physical Chemistry B*, 110(50):25371–25382, Dec 2006. ISSN 1520-6106. doi:10.1021/jp0644816. URL <https://doi.org/10.1021/jp0644816>.
- [176] Vanessa M. Huxter, Jeongho Kim, Shun S. Lo, Anna Lee, Sreekumari P. Nair, and Gregory D. Scholes. Spin relaxation in zinc blende and wurtzite cdse quantum dots. *Chemical Physics Letters*, 491(4):187–192, 2010. ISSN 0009-2614. doi:<https://doi.org/10.1016/j.cplett.2010.03.081>. URL <https://www.sciencedirect.com/science/article/pii/S0009261410004926>.
- [177] Ryan W. Crisp, Joel N. Schrauben, Matthew C. Beard, Joseph M. Luther, and Justin C. Johnson. Coherent exciton delocalization in strongly coupled quantum dot arrays. *Nano Letters*, 13(10):4862–4869, Oct 2013. ISSN 1530-6984. doi:10.1021/nl402725m. URL <https://doi.org/10.1021/nl402725m>.
- [178] A. R. Cameron, P. Riblet, and A. Miller. Spin gratings and the measurement of electron drift mobility in multiple quantum well semiconductors. *Phys. Rev. Lett.*, 76:4793–4796, Jun 1996. doi:10.1103/PhysRevLett.76.4793. URL <https://link.aps.org/doi/10.1103/PhysRevLett.76.4793>.
- [179] C. P. Weber, J. Orenstein, B. Andrei Bernevig, Shou-Cheng Zhang, Jason Stephens, and D. D. Awschalom. Nondiffusive spin dynamics in a two-dimensional electron gas. *Phys. Rev. Lett.*, 98:076604, Feb 2007. doi:10.1103/PhysRevLett.98.076604. URL <https://link.aps.org/doi/10.1103/PhysRevLett.98.076604>.
- [180] Jing Wang, Yang Guo, Yuan Huang, Hailan Luo, Xingjiang Zhou, Changzhi Gu, and Baoli Liu. Diffusion dynamics of valley excitons by transient grating spectroscopy in monolayer wse₂. *Applied Physics Letters*, 115(13):131902, 09 2019. ISSN 0003-6951. doi:10.1063/1.5116263. URL <https://doi.org/10.1063/1.5116263>.

- [181] Henning Kuhn, Julian Wagner, Shuangping Han, Robin Bernhardt, Yan Gao, Liantuan Xiao, Jingyi Zhu, and Paul H. M. van Loosdrecht. Excitonic transport and intervalley scattering dynamics in large-size exfoliated mose₂ monolayer investigated by heterodyned transient grating spectroscopy. *Laser & Photonics Reviews*, 14(12):2000029, 2020. doi: <https://doi.org/10.1002/lpor.202000029>. URL <https://onlinelibrary.wiley.com/doi/abs/10.1002/lpor.202000029>.
- [182] Navaneetha K. Ravichandran, Hang Zhang, and Austin J. Minnich. Spectrally resolved specular reflections of thermal phonons from atomically rough surfaces. *Phys. Rev. X*, 8: 041004, Oct 2018. doi:10.1103/PhysRevX.8.041004. URL <https://link.aps.org/doi/10.1103/PhysRevX.8.041004>.
- [183] Chun-Mao Li, Theodore Sjodin, and Hai-Lung Dai. Photoexcited carrier diffusion near a si(111) surface: Non-negligible consequence of carrier-carrier scattering. *Phys. Rev. B*, 56: 15252–15255, Dec 1997. doi:10.1103/PhysRevB.56.15252. URL <https://link.aps.org/doi/10.1103/PhysRevB.56.15252>.
- [184] A. A. Maznev, Jeremy A. Johnson, and Keith A. Nelson. Onset of nondiffusive phonon transport in transient thermal grating decay. *Phys. Rev. B*, 84:195206, Nov 2011. doi: 10.1103/PhysRevB.84.195206. URL <https://link.aps.org/doi/10.1103/PhysRevB.84.195206>.
- [185] A. J. Minnich. Determining phonon mean free paths from observations of quasiballistic thermal transport. *Phys. Rev. Lett.*, 109:205901, Nov 2012. doi:10.1103/PhysRevLett.109.205901. URL <https://link.aps.org/doi/10.1103/PhysRevLett.109.205901>.
- [186] Fan Yang and Chris Dames. Mean free path spectra as a tool to understand thermal conductivity in bulk and nanostructures. *Phys. Rev. B*, 87:035437, Jan 2013. doi: 10.1103/PhysRevB.87.035437. URL <https://link.aps.org/doi/10.1103/PhysRevB.87.035437>.
- [187] Gang Chen. Non-fourier phonon heat conduction at the microscale and nanoscale. *Nature Reviews Physics*, 3(8):555–569, Aug 2021. ISSN 2522-5820. doi:10.1038/s42254-021-00334-1. URL <https://doi.org/10.1038/s42254-021-00334-1>.
- [188] Taeyong Kim, Stavros X. Drakopoulos, Sara Ronca, and Austin J. Minnich. Origin of high thermal conductivity in disentangled ultra-high molecular weight polyethylene films: ballistic phonons within enlarged crystals. *Nature Communications*, 13(1):2452, May

2022. ISSN 2041-1723. doi:10.1038/s41467-022-29904-2. URL <https://doi.org/10.1038/s41467-022-29904-2>.
- [189] Motowo Takayanagi, Shinsaku Uemura, and Shunsuke Minami. Application of equivalent model method to dynamic rheo-optical properties of crystalline polymer. *Journal of Polymer Science Part C: Polymer Symposia*, 5(1):113–122, 1964. doi: <https://doi.org/10.1002/polc.5070050111>. URL <https://onlinelibrary.wiley.com/doi/abs/10.1002/polc.5070050111>.
- [190] C.L. Choy and K. Young. Thermal conductivity of semicrystalline polymers — a model. *Polymer*, 18(8):769–776, 1977. ISSN 0032-3861. doi:[https://doi.org/10.1016/0032-3861\(77\)90179-3](https://doi.org/10.1016/0032-3861(77)90179-3). URL <https://www.sciencedirect.com/science/article/pii/0032386177901793>.
- [191] Tingyu Lu, Kyunghoon Kim, Xiaobo Li, Jun Zhou, Gang Chen, and Jun Liu. Thermal transport in semicrystalline polyethylene by molecular dynamics simulation. *Journal of Applied Physics*, 123(1):015107, 01 2018. ISSN 0021-8979. doi:10.1063/1.5006889. URL <https://doi.org/10.1063/1.5006889>.
- [192] Sara Ronca, Tamito Igarashi, Giuseppe Forte, and Sanjay Rastogi. Metallic-like thermal conductivity in a lightweight insulator: Solid-state processed ultra high molecular weight polyethylene tapes and films. *Polymer*, 123:203–210, 2017. ISSN 0032-3861. doi:<https://doi.org/10.1016/j.polymer.2017.07.027>. URL <https://www.sciencedirect.com/science/article/pii/S0032386117306869>.
- [193] Yanfei Xu, Daniel Kraemer, Bai Song, Zhang Jiang, Jiawei Zhou, James Loomis, Jianjian Wang, Mingda Li, Hadi Ghasemi, Xiaopeng Huang, Xiaobo Li, and Gang Chen. Nanostructured polymer films with metal-like thermal conductivity. *Nature Communications*, 10(1):1771, Apr 2019. ISSN 2041-1723. doi:10.1038/s41467-019-09697-7. URL <https://doi.org/10.1038/s41467-019-09697-7>.
- [194] F. Bencivenga, R. Cucini, F. Capotondi, A. Battistoni, R. Mincigrucci, E. Giangrisostomi, A. Gessini, M. Manfredda, I. P. Nikolov, E. Pedersoli, E. Principi, C. Svetina, P. Parisse, F. Casolari, M. B. Danailov, M. Kiskinova, and C. Masciovecchio. Four-wave mixing experiments with extreme ultraviolet transient gratings. *Nature*, 520(7546):205–208, Apr 2015. ISSN 1476-4687. doi:10.1038/nature14341. URL <https://doi.org/10.1038/nature14341>.
- [195] F. Bencivenga, R. Mincigrucci, F. Capotondi, L. Foglia, D. Naumenko, A. A. Maznev, E. Pedersoli, A. Simoncig, F. Caporaletti, V. Chiloyan, R. Cucini, F. Dallari, R. A. Duncan, T. D.

- Frazer, G. Gaio, A. Gessini, L. Giannessi, S. Huberman, H. Kapteyn, J. Knobloch, G. Kurdi, N. Mahne, M. Manfredda, A. Martinelli, M. Murnane, E. Principi, L. Raimondi, S. Spampinati, C. Spezzani, M. Trovò, M. Zangrando, G. Chen, G. Monaco, K. A. Nelson, and C. Masciovecchio. Nanoscale transient gratings excited and probed by extreme ultraviolet femtosecond pulses. *Science Advances*, 5(7):eaaw5805, 2019. doi:10.1126/sciadv.aaw5805. URL <https://www.science.org/doi/abs/10.1126/sciadv.aaw5805>.
- [196] Peter R. Miedaner, Nadia Berndt, Jude Deschamps, Sergei Urazhdin, Nupur Khatu, Danny Fainozzi, Marta Brioschi, Pietro Carrara, Riccardo Cucini, Giorgio Rossi, Steffen Witrock, Dmitriy Ksenzov, Riccardo Mincigrucci, Filippo Bencivenga, Laura Foglia, Ettore Paltanin, Stefano Bonetti, Dieter Engel, Daniel Schick, Christian Gutt, Riccardo Comin, Keith A. Nelson, and Alexei A. Maznev. Excitation and detection of coherent nanoscale spin waves via extreme ultraviolet transient gratings. *Science Advances*, 10(36):eadp6015, 2024. doi:10.1126/sciadv.adp6015. URL <https://www.science.org/doi/abs/10.1126/sciadv.adp6015>.
- [197] Jérémie R. Rouxel, Danny Fainozzi, Roman Mankowsky, Benedikt Rösner, Gediminas Seniutinas, Riccardo Mincigrucci, Sara Catalini, Laura Foglia, Riccardo Cucini, Florian Döring, Adam Kubec, Frieder Koch, Filippo Bencivenga, Andre Al Haddad, Alessandro Gessini, Alexei A. Maznev, Claudio Cirelli, Simon Gerber, Bill Pedrini, Giulia F. Mancini, Elia Razzoli, Max Burian, Hiroki Ueda, Georgios Pamfilidis, Eugenio Ferrari, Yunpei Deng, Aldo Mozzanica, Philip J. M. Johnson, Dmitry Ozerov, Maria Grazia Izzo, Cettina Bottari, Christopher Arrell, Edwin James Divall, Serhane Zerdane, Mathias Sander, Gregor Knopp, Paul Beaud, Henrik T. Lemke, Chris J. Milne, Christian David, Renato Torre, Majed Chergui, Keith A. Nelson, Claudio Masciovecchio, Urs Staub, Luc Patthey, and Cristian Svetina. Hard x-ray transient grating spectroscopy on bismuth germanate. *Nature Photonics*, 15(7):499–503, Jul 2021. ISSN 1749-4893. doi:10.1038/s41566-021-00797-9. URL <https://doi.org/10.1038/s41566-021-00797-9>.
- [198] Ashley P. Fidler, Seth J. Camp, Erika R. Warrick, Etienne Bloch, Hugo J. B. Marroux, Daniel M. Neumark, Kenneth J. Schafer, Mette B. Gaarde, and Stephen R. Leone. Nonlinear xuv signal generation probed by transient grating spectroscopy with attosecond pulses. *Nature Communications*, 10(1):1384, Mar 2019. ISSN 2041-1723. doi:10.1038/s41467-019-09317-4. URL <https://doi.org/10.1038/s41467-019-09317-4>.

- [199] Rafael Quintero-Bermudez, Lauren Drescher, Vincent Eggers, Kevin Gulu Xiong, and Stephen R. Leone. Attosecond transient grating spectroscopy with near-infrared grating pulses and an extreme ultraviolet diffracted probe. *ACS Photonics*, 12(4):2097–2105, 2025. doi: 10.1021/acsphotonics.4c02545. URL <https://doi.org/10.1021/acsphotonics.4c02545>.
- [200] Andrey Kobyakov, Michael Sauer, and Dipak Chowdhury. Stimulated brillouin scattering in optical fibers. *Adv. Opt. Photon.*, 2(1):1–59, Mar 2010. doi:10.1364/AOP.2.000001. URL <https://opg.optica.org/aop/abstract.cfm?URI=aop-2-1-1>.
- [201] C. Wolff, M. J. Steel, B. J. Eggleton, and C. G. Poulton. Stimulated brillouin scattering in integrated photonic waveguides: Forces, scattering mechanisms, and coupled-mode analysis. *Phys. Rev. A*, 92:013836, Jul 2015. doi:10.1103/PhysRevA.92.013836. URL <https://link.aps.org/doi/10.1103/PhysRevA.92.013836>.
- [202] Roel Botter, Kaixuan Ye, Yvan Klaver, Radius Suryadharma, Okky Daulay, Gaojian Liu, Jasper van den Hoogen, Lou Kanger, Peter van der Slot, Edwin Klein, Marcel Hoekman, Chris Roeloffzen, Yang Liu, and David Marpaung. Guided-acoustic stimulated brillouin scattering in silicon nitride photonic circuits. *Science Advances*, 8(40):eabq2196, 2022. doi:10.1126/sciadv.abq2196. URL <https://www.science.org/doi/abs/10.1126/sciadv.abq2196>.
- [203] Govert Neijts, Choon Kong Lai, Maren Kramer Riseng, Duk-Yong Choi, Kunlun Yan, David Marpaung, Stephen J. Madden, Benjamin J. Eggleton, and Moritz Merklein. On-chip stimulated brillouin scattering via surface acoustic waves. *APL Photonics*, 9(10):106114, 10 2024. ISSN 2378-0967. doi:10.1063/5.0220496. URL <https://doi.org/10.1063/5.0220496>.
- [204] Kaixuan Ye, Akshay Keloth, Yisbel E. Marin, Matteo Cherchi, Timo Aalto, and David Marpaung. Stimulated brillouin scattering in a non-suspended ultra-low-loss thick-soi platform. *APL Photonics*, 10(2):026108, 02 2025. ISSN 2378-0967. doi:10.1063/5.0246281. URL <https://doi.org/10.1063/5.0246281>.
- [205] Giuliano Scarcelli and Seok Hyun Yun. Confocal brillouin microscopy for three-dimensional mechanical imaging. *Nature Photonics*, 2(1):39–43, Jan 2008. ISSN 1749-4893. doi: 10.1038/nphoton.2007.250. URL <https://doi.org/10.1038/nphoton.2007.250>.
- [206] Giuliano Scarcelli and Seok Hyun Yun. In vivo brillouin optical microscopy of the human eye. *Opt. Express*, 20(8):9197–9202, Apr 2012. doi:10.1364/OE.20.009197. URL <https://opg.optica.org/oe/abstract.cfm?URI=oe-20-8-9197>.

- [207] Giuliano Scarcelli, Sabine Kling, Elena Quijano, Roberto Pineda, Susana Marcos, and Seok Hyun Yun. Brillouin microscopy of collagen crosslinking: Noncontact depth-dependent analysis of corneal elastic modulus. *Investigative Ophthalmology & Visual Science*, 54(2):1418–1425, 02 2013. ISSN 1552-5783. doi:10.1167/iovs.12-11387. URL <https://doi.org/10.1167/iovs.12-11387>.
- [208] Giuseppe Antonacci, Valeria de Turris, Alessandro Rosa, and Giancarlo Ruocco. Background-deflection brillouin microscopy reveals altered biomechanics of intracellular stress granules by als protein fus. *Communications Biology*, 1(1):139, Sep 2018. ISSN 2399-3642. doi: 10.1038/s42003-018-0148-x. URL <https://doi.org/10.1038/s42003-018-0148-x>.
- [209] Giuliano Scarcelli, William J. Polacheck, Hadi T. Nia, Kripa Patel, Alan J. Grodzinsky, Roger D. Kamm, and Seok Hyun Yun. Noncontact three-dimensional mapping of intracellular hydromechanical properties by brillouin microscopy. *Nature Methods*, 12(12):1132–1134, Dec 2015. ISSN 1548-7105. doi:10.1038/nmeth.3616. URL <https://doi.org/10.1038/nmeth.3616>.
- [210] Peng Shao, Amira M. Eltony, Theo G. Seiler, Behrouz Tavakol, Roberto Pineda, Tobias Koller, Theo Seiler, and Seok-Hyun Yun. Spatially-resolved brillouin spectroscopy reveals biomechanical abnormalities in mild to advanced keratoconus in vivo. *Scientific Reports*, 9(1):7467, May 2019. ISSN 2045-2322. doi:10.1038/s41598-019-43811-5. URL <https://doi.org/10.1038/s41598-019-43811-5>.
- [211] Irina Kabakova, Jitao Zhang, Yuchen Xiang, Silvia Caponi, Alberto Bilenca, Jochen Guck, and Giuliano Scarcelli. Brillouin microscopy. *Nature Reviews Methods Primers*, 4(1):8, Feb 2024. ISSN 2662-8449. doi:10.1038/s43586-023-00286-z. URL <https://doi.org/10.1038/s43586-023-00286-z>.
- [212] Pierre Bouvet, Carlo Bevilacqua, Yogeshwari Ambekar, Giuseppe Antonacci, Joshua Au, Silvia Caponi, Sophie Chagnon-Lessard, Juergen Czarske, Thomas Dehoux, Daniele Fioretto, Yujian Fu, Jochen Guck, Thorsten Hamann, Dag Heinemann, Torsten Jähnke, Hubert Jean-Ruel, Irina Kabakova, Kristie Koski, Nektarios Koukourakis, David Krause, Salvatore La Cava-
era, Timm Landes, Jinha Li, Hadi Mahmodi, Jeremie Margueritat, Maurizio Mattarelli, Michael Monaghan, Darryl R. Overby, Fernando Perez-Cota, Emanuele Pontecorvo, Robert Prevedel, Giancarlo Ruocco, John Sandercock, Giuliano Scarcelli, Filippo Scarponi, Claudia Testi, Peter Török, Lucie Vovard, Wolfgang J. Weninger, Vladislav Yakovlev, Seok-Hyun

Yun, Jitao Zhang, Francesca Palombo, Alberto Bilenca, and Kareem Elsayad. Consensus statement on brillouin light scattering microscopy of biological materials. *Nature Photonics*, 19(7):681–691, Jul 2025. ISSN 1749-4893. doi:10.1038/s41566-025-01681-6. URL <https://doi.org/10.1038/s41566-025-01681-6>.